University of South-Eastern Norway

www.usn.no

FMH606 Master's Thesis 2022
Process Technology

Theoretical analysis of pipe flow during liquid hydrogen bunkering

Nils Jørgen Aavik

Faculty of Technology, Natural Sciences and Maritime Sciences
Campus Porsgrunn

University of South-Eastern Norway

www.usn.no

Course: FMH606 Master's Thesis 2022
Title: *Theoretical analysis of pipe flow during liquid hydrogen bunkering*
Pages: *60*
Keywords: *Liquid hydrogen, bunkering, pipe flow, pressure loss, phase analysis*

Student: *Nils Jørgen Aavik*
Supervisor: *Knut Vågsæther*
External partner: *KPN H2Maritime*

Summary:
This thesis aimed to use theoretical models to estimate the pressure loss in liquid hydrogen bunkering and to study the phase of hydrogen through the system. Mass flow is studied as well, using two methods of curve fitting and a calculation model for mass flow out of a nozzle. Current bunkering technology is presented briefly.

The Norwegian Defence Research Establishment's experiments on outdoor and indoor releases of liquid hydrogen has formed the basis of the model work. A Helmholtz EOS solver is used to determine the thermodynamic states and key parameters in the system, and to predict the phase of hydrogen. A standard pressure loss model with the Darcy-Weisbach equation is used.

The work on mass flow displays calculated values close to provided data at higher mass flows. The pressure loss model shows varying accuracy when compared to the measured data, but the calculated values are within ±15-25% at higher pressure. The phase analysis shows that hydrogen will start to boil only after a few seconds of starting the bunkering.

Preface

First, I would like to thank my supervisor, Knut Vågsæther, for great insight, motivation and expertise during the making of this thesis.

I would also like to thank my father, Geir Egil Aavik, for his much appreciated help with improving the language quality of my thesis.

Lastly, I would like to thank my family and my partner for their positive encouragement and for always cheering me on.

Porsgrunn, 18th May 2022

Nils Jørgen Aavik

Contents

Preface **4**

Contents **6**

1 Introduction **8**
1.1 Liquid hydrogen in maritime industry . . . 9
1.2 Aim . . . 10

2 Background **11**
2.1 Why liquid hydrogen? . . . 11
2.2 FFI's experimental work . . . 11
2.2.1 Description of experiments . . . 12
2.2.2 Equipment . . . 13
2.2.3 Results from tests 1-4 . . . 14
2.3 Important parameters in liquid hydrogen use . . . 18
2.3.1 Pressure and temperature . . . 18
2.4 Two-phase flow . . . 19
2.5 Safety challenges . . . 21
2.5.1 Fire and explosions . . . 21
2.5.2 Cryogenic burns . . . 21
2.5.3 Hydrogen embrittlement . . . 21
2.5.4 Confined spaces . . . 22

3 Current bunkering technology **23**
3.1 Bunkering methods . . . 23
3.1.1 Ship-to-ship . . . 23
3.1.2 Shore-to-ship . . . 25
3.1.3 Truck-to-ship . . . 26
3.2 System . . . 27
3.2.1 Production . . . 28
3.2.2 Liquefaction of hydrogen . . . 28
3.2.3 Bunkering equipment . . . 29

4 Method **31**
4.1 Pressure loss model . . . 31

4.2 Helmholtz EOS . . . 33
4.2.1 Hydrogen parameters and state definition . . . 34
4.2.2 Hydrogen phase in the system . . . 34
4.3 Mass flow model . . . 35
4.4 Model for nozzle mass flow . . . 35

5 Results **38**
5.1 Analysis of FFI's experiments . . . 38
5.1.1 System pressure . . . 38
5.1.2 System temperature . . . 39
5.2 Mass flow . . . 40
5.3 Pressure loss calculation . . . 42
5.4 End nozzle analysis . . . 46
5.5 Phase analysis . . . 47

6 Discussion **51**
6.1 Model validity . . . 51
6.1.1 Pressure loss model . . . 51
6.1.2 Helmholtz EOS . . . 52
6.1.3 Mass flow- and nozzle model . . . 52
6.2 Hydrogen phase discussion . . . 52
6.3 Aspects of a bunkering scenario . . . 52
6.3.1 Production . . . 52
6.3.2 Bunkering method . . . 53
6.3.3 Bunkering system . . . 53
6.3.4 Pressure loss in tanker . . . 53
6.3.5 Pump vs pressure difference . . . 55
6.4 Missing knowledge . . . 55

7 Conclusion **56**

References **57**

A Models **60**
A.1 Script with Helmholtz EOS . . . 60
A.2 Phase analyser . . . 60
A.3 Script for mass flow- and pressure calculation (Tests 1-4) . . . 60
A.4 Excel documents read by Python (Test 1-4) . . . 60
A.5 Nozzle calculator . . . 60

Nomenclature

Symbol	Explanation
Bar	Absolute pressure
Barg	Gauge pressure
Boil-off	Loss of liquid due to boiling
Bunkering	The process of fueling a ship
CO_2	Carbon dioxide
CRBJT	Combined-reversed-Brayton-Joule-Thompson
Isentalpic	Thermodynamic process with no change in enthalpy
FFI	Norwegian Defence Research Establishment
K	Kelvin
kPa	Kilo Pascal
LH2	Liquid hydrogen
LNG	Liquefied natural gas
MF	Mass flow
NB	Nominal bore
Pascal	Unit of pressure
P-V diagram	Pressure vs Volume diagram

1 Introduction

Energy is the driving force of today's society. It powers our homes, our cars and is a vital part in all industry. With increasing population and higher living standards, the need for energy continues to rise in line with global emissions. The continued use of fossil fuels are threatening the Earth's climate with increasing temperatures and rising sea levels. A world wide transition to renewable energy and green technology is required to continue life as it is today. The three main sources of energy in the world continue to be oil, natural gas and coal [1]. These hydrocarbon fuels release massive amounts of greenhouse gases when used to produce energy, for example through a burning process. Many different substances are released during energy production with fossil fuels, such as NO_x, sulfur dioxide and CO_2, to name a few [2]. These substances affect the environment negatively by pollution of drinking water, acid rain and heating of the atmosphere. Figure 1.1 shows the primary energy consumption in the world in 2021.

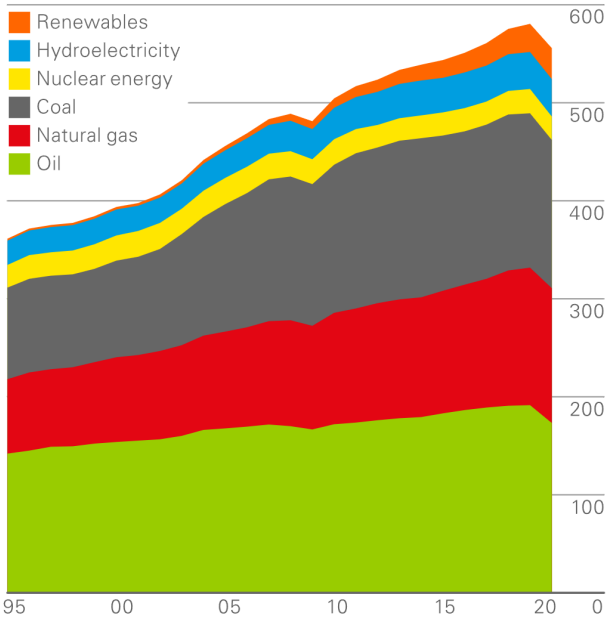

Figure 1.1: Primary energy consumption in the world [1]

Due to the environmental damage caused by the use of hydrocarbons for energy, a transition to cleaner energy is needed. This is already happening in many parts of the world, with increasing number of wind- and solar farms, building of hydroelectric power plants

and more research into low-carbon alternatives. Different energy carriers are also an important part of the shift to green energy. An energy carrier is defined by ISO 13600 as: "Substance or phenomenon that can be used to produce mechanical work or heat or to operate chemical or physical processes." [3], meaning that the substance don't produce energy but *contains* it. Some examples of energy carriers are electricity, gasoline, diesel, natural gas and hydrogen. This report will focus on the latter, more specifically liquid hydrogen.

1.1 Liquid hydrogen in maritime industry

According to the European Maritime Transport Environmental Report (EMTER) published by the European Maritime Safety Agency and the European Environment Agency, maritime transport handles 77% of the EU's external- and 35% of the internal trade [4]. It is one of the most important factors in the EU's supply chain. Maritime transport contributes between 2-3% of annual carbon dioxide emission, which in 2018 was 1056 million tonnes of CO_2 [5]. Emissions related to maritime transport are mainly due to the use of diesel-powered cargo ships. To uphold the Paris climate agreement of keeping the Earth's temperature increase below 2°, low emission fuels must be adopted by the transport industry. One of the fuels considered is the use of liquid hydrogen.

Liquid hydrogen is an ideal energy carrier for maritime transport. The only by-product is water, the storage in liquid phase increases the ships fuel capacity considerably compared to gas-phase, and it is versatile in terms of extracting energy. Much of the technology associated with LNG can also be used with slight adjustments. To fuel a ship with liquid hydrogen (bunkering) three main components are required:

1. A way to transport the hydrogen from production plant to port, usually a transport truck.
2. Pre-cooled piping system for transfer between truck and ship
3. Either a pressure difference between transfer tank and receiving tank, or a pump.

The most common way to transport liquid fuel (LNG, diesel, gasoline etc.) to ports, is by tank truck. A truck can typically carry around 40 000 liters of liquid fuel. In use with liquid hydrogen, the tank and piping must be vacuum insulated, pre-cooled and purged before carrying hydrogen. It is also common to have a self pressurization system using boil-off gas. A piping system designed for cryo-fluids must be used to transfer liquid hydrogen. To transfer the hydrogen from truck to ship, a pressure difference or a pump is used.

1.2 Aim

This report aims to evaluate current technology for bunkering liquid hydrogen and to analyse experiments conducted by FFI to further understand the mechanics of pressure, temperature, and mass flow in a bunkering system. To investigate the pressure loss in a bunkering system, a standard pressure loss calculation will be preformed and compared to experimental data. A Helmholtz EOS solver will be used to determine the thermodynamic states, provide parameters and to investigate the phase of hydrogen through a bunkering system. Furthermore, the mass flow in a pipe system with liquid hydrogen is analysed using measured data and a nozzle model.

2 Background

2.1 Why liquid hydrogen?

Hydrogen has received much attention over the last decade as a clean energy carrier. Hydrogen is the simplest of all atoms and the first element in the periodic table. It is the most abundant element on earth and usually doesn't exist on its own but rather in compounds such as water (H_2O) or in hydrocarbons such as CH_4. Production of hydrogen gas from these compounds are typically done by steam-methane reforming or by water electrolysis [6]. One of the reasons hydrogen is a sought-after energy carrier, is its large energy density of approximately 120 megajoules per kilogram (MJ/kg). In contrast, the energy density of diesel is 45.5 MJ/kg. This means that carrying the same amount of hydrogen compared to diesel gives about 2.6 times the energy per kg. Another reason to use hydrogen is the versatility it brings when being used. Hydrogen can be burned in slightly modified, already existing LNG combustion engines to produce mechanical work and heat [7], or be used in a fuel cell to produce electricity and heat with only water as the chemical product [8].

A downside to using hydrogen as an energy carrier is the low density of 0.083 kg/m^3 at room temperature and atmospheric pressure. It needs to be either pressurized or liquefied to carry enough fuel to be used in cars and ships. Hydrogen cars today typically use gas-phase hydrogen pressurized to between 350 and 700 bars, achieving ranges comparable to diesel and gasoline cars. Using gaseous hydrogen is not sufficient for propelling large ships traveling thousands of nautical miles due to the large storage tanks required. Here, a solution using liquid hydrogen is more favorable.

2.2 FFI's experimental work

In December 2019 and January 2020, DNV GL Spadeadam Research and Testing conducted a series of indoor- and outdoor release tests with liquid hydrogen. The goal was to better understand the mechanisms in a liquid hydrogen release and improve upon existing models for risk assessment. The Norwegian Directorate for Civil Protection (DSB) and the Norwegian Maritime Authority have categorized this as an area of limited knowledge

[9]. In this report, only the outdoor release experiments will be considered in detail. Furthermore, mainly the pressure sensor data is of interest in this work, but some general safety concerns are presented in 2.5.

This chapter is a reproduction of DNV and FFI's report "Large scale leakage of liquid hydrogen (LH2)-tests related to bunkering and maritime use of liquid hydrogen". The material presented in this chapter is the parts of the report considered valuable for this work. For the full report see reference [10].

2.2.1 Description of experiments

The setup for the experiments consisted of real-scale bunkering dimensions in terms of required space, as well as the tanker truck used, piping, and piping equipment. The pipes were fitted with pressure- and temperature sensors to monitor the liquid hydrogen. The mass flow was measured by weighing the tank truck during release to calculate the flow. The flow rates used were similar to that of a real bunkering scenario as well as pre-cooling and purging of equipment before use. Figure 2.1 shows a schematic layout of the experimental setup.

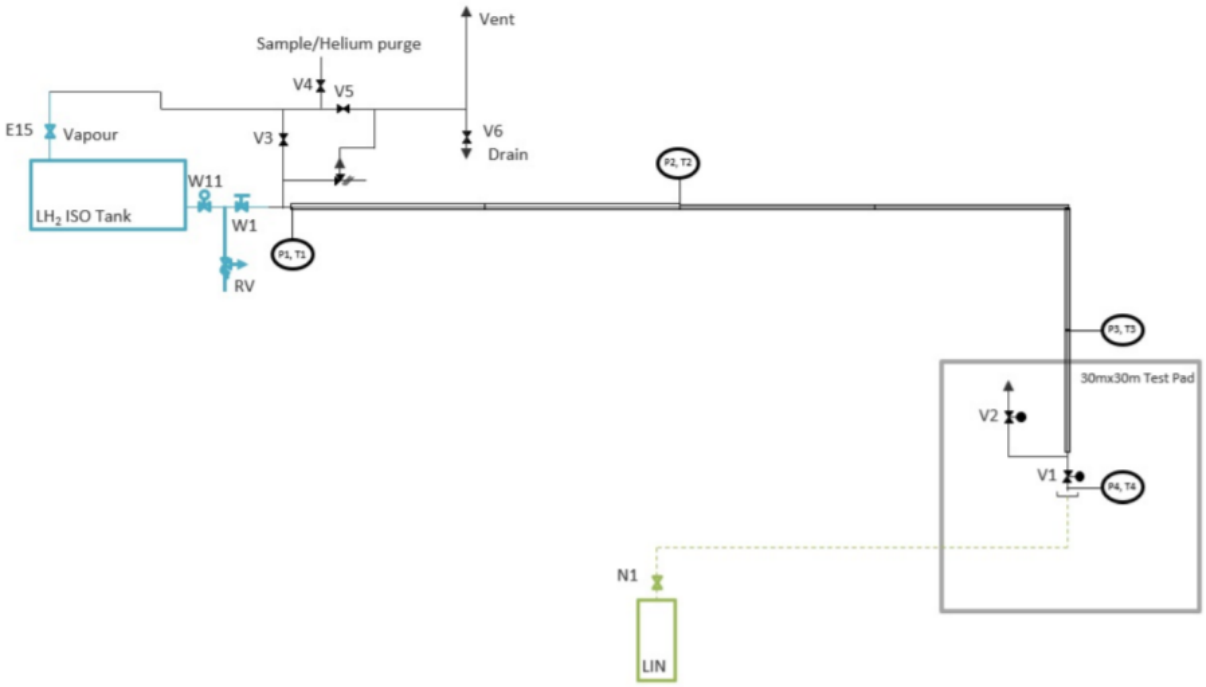

Figure 2.1: Experimental setup [9]

A total of 7 outdoor- and 8 indoor release experiments were conducted in FFI's work, both unignited- and ignited releases. The main parts of this report will focus on tests 1-4 as they differ in initial pressure and mass flow rates, but the remaining 3 outdoor tests and the indoor experiments will be briefly mentioned in section 2.5. Experiments 1-4 are summarized in table 2.1.

Table 2.1: Summary of experiments [9]

Test no	Initial tanker pressure (barg)	Mass flow (kg/min)	Run time (min)	Release orientation
1	2	13.5	13	Vertical downwards
2	6	28.2	8	Vertical downwards
3	10	43.8	15	Vertical downwards
4	10	49.7	6	Horizontal downwards

2.2.2 Equipment

Piping

The piping setup in the experiments consisted of 42 meters of piping where each length was 6 meters. Flanges were used to attach each pipe to the next. The pipe had an inner 2"NB pipe with a larger 4"NB jacket on the outside, complete with flexible tubing in the same size. All piping was 316L stainless steel. The space between the pipes was filled with perlite and a vacuum was applied. A vacuum between the inner and outer pipe ensures a very low thermal conductivity.

Measurements

Four locations along the piping were fitted with pressure- and temperature sensors. The pressure was measured using a Druck UNIK 5000 pressure transducer with a range of 0-16 barg and accuracy of $\pm 0.04\%$, quoted by the manufacturer. The temperature was measured using a stainless steel sheathed, mineral insulated Type "T" 1.5 mm thermocouples.

2.2.3 Results from tests 1-4

This section presents the results from the 4 tests considered.

Test 1

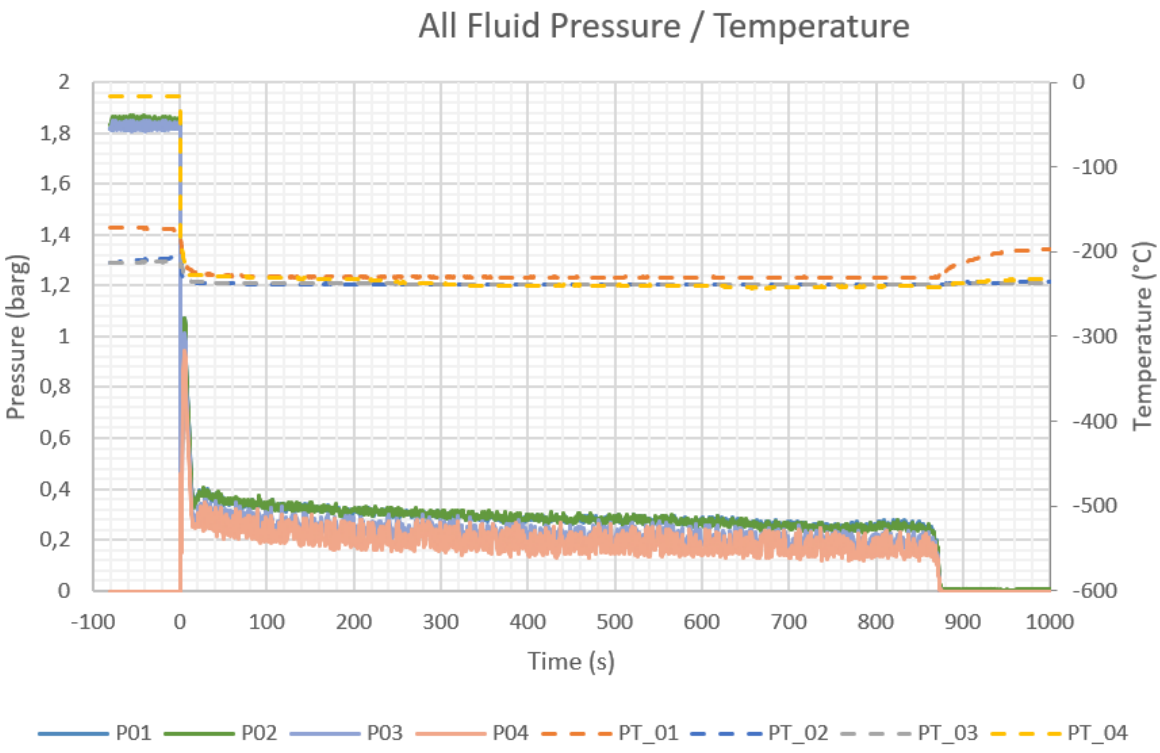

Figure 2.2: Results from test 1 [10]

Figure 2.2 shows the pressure- and temperature development with time during test 1. The pressure drops significantly in the beginning and continues to drop slowly with time. Each sensor follows the same trend after around $t = 20$ seconds. Between $t = 20$ and $t = 850$, the pressure measurements fluctuates between 0.2 and 0.4 barg. The temperature remains constant throughout most of the experiment, except at the beginning and at the end.

Test 2

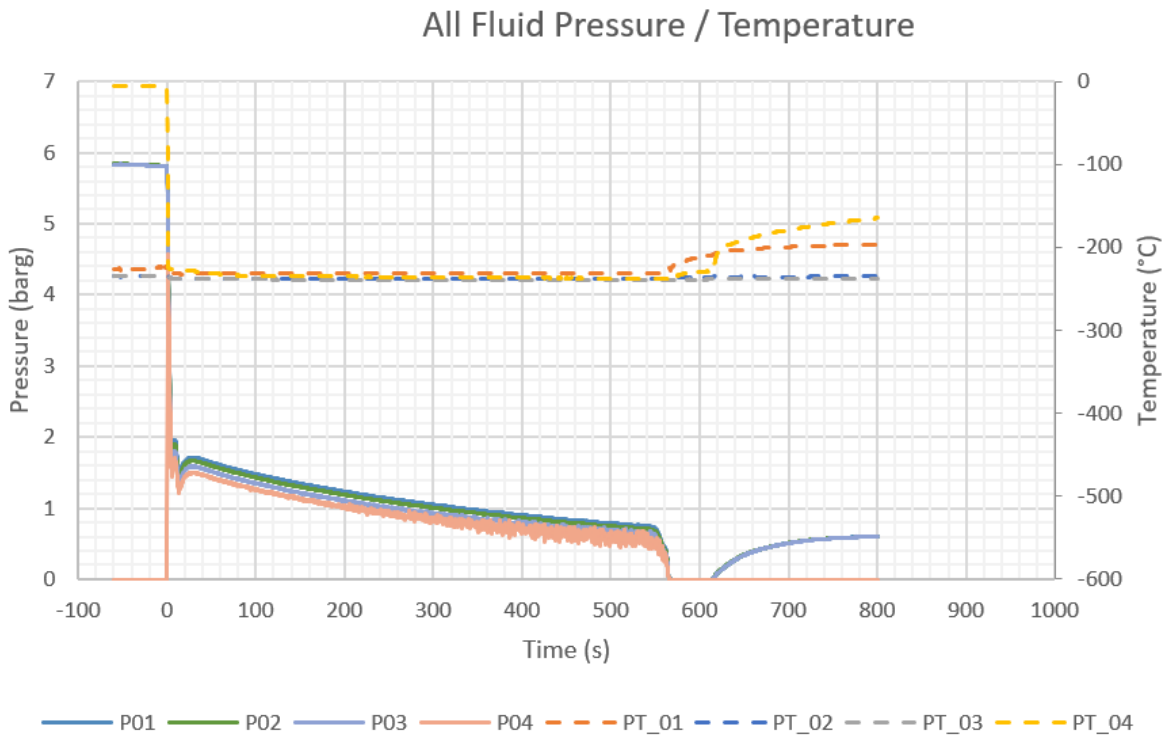

Figure 2.3: Results from test 2 [10]

Pressure- and temperature development in test 2 is shown in figure 2.3. Here, as in test 1, the temperature remains constant other than at the start and finish. The pressure is also similar, with a large pressure drop at the beginning with a continued decrease in pressure with time. Fluctuating measurements are lower in this test.

Test 3

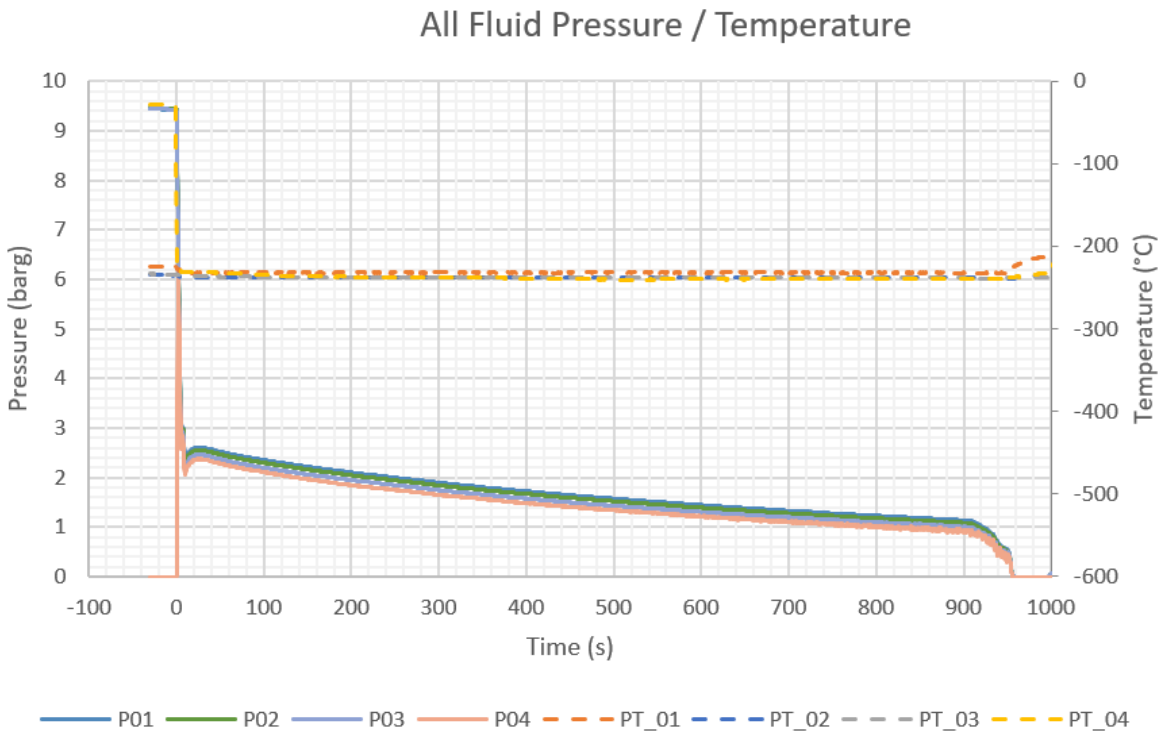

Figure 2.4: Results from test 3 [10]

As in tests 1 and 2, the trend of test 3 is similar with constant temperature during most of the experiment and a large pressure drop at the beginning followed by an almost linear decrease in pressure. Fluctuations are mostly gone in this test. Figure 2.4 shows the plot.

Test 4

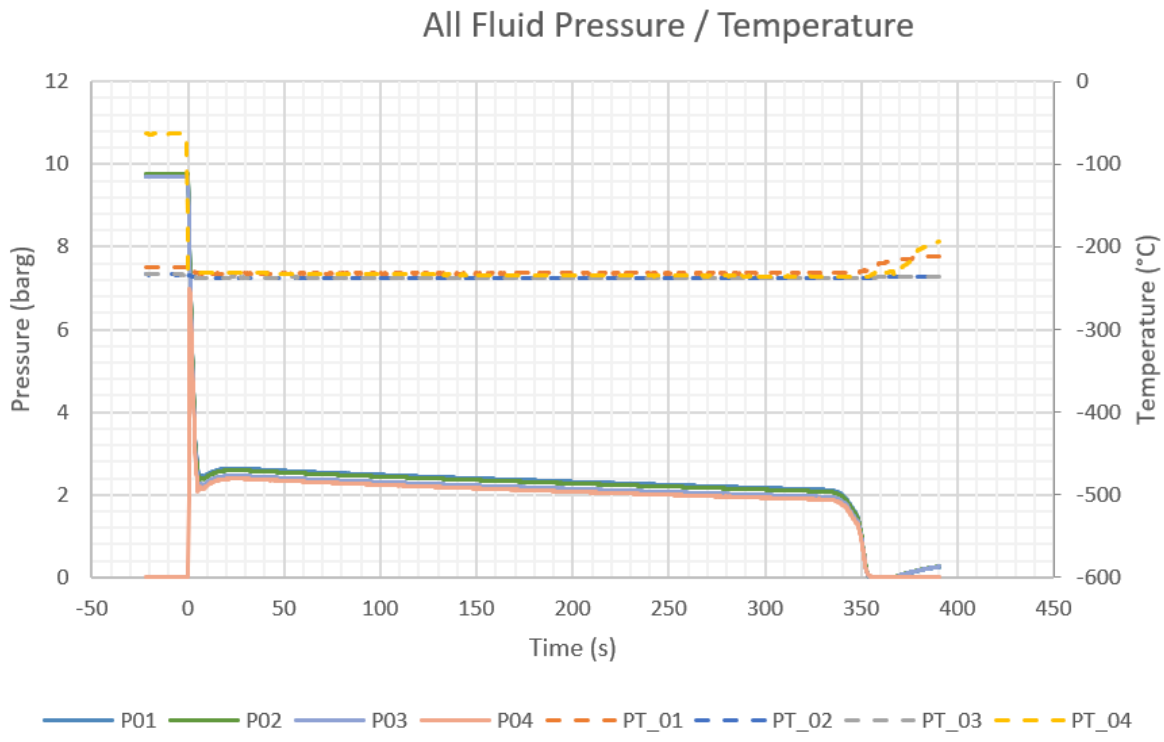

Figure 2.5: Results from test 4 [10]

Figure 2.5 shows test 4, which displays the same trends as the other tests. This test varies slightly in that the pressure decrease, after the initial large drop, is less than in tests 1-3.

2.3 Important parameters in liquid hydrogen use

2.3.1 Pressure and temperature

When a fluid flows through a pipe, it must overcome the friction exerted by the walls. This will cause a reduction in pressure. Temperature is also a critical parameter as it must be kept sufficiently low to avoid boiling. In liquid hydrogen applications, this is critical due to the nature of phase transfer. The combination of pressure and temperature where liquid hydrogen can exist, makes up a small region of the phase diagram. Figure 2.6 shows the phase diagram for hydrogen.

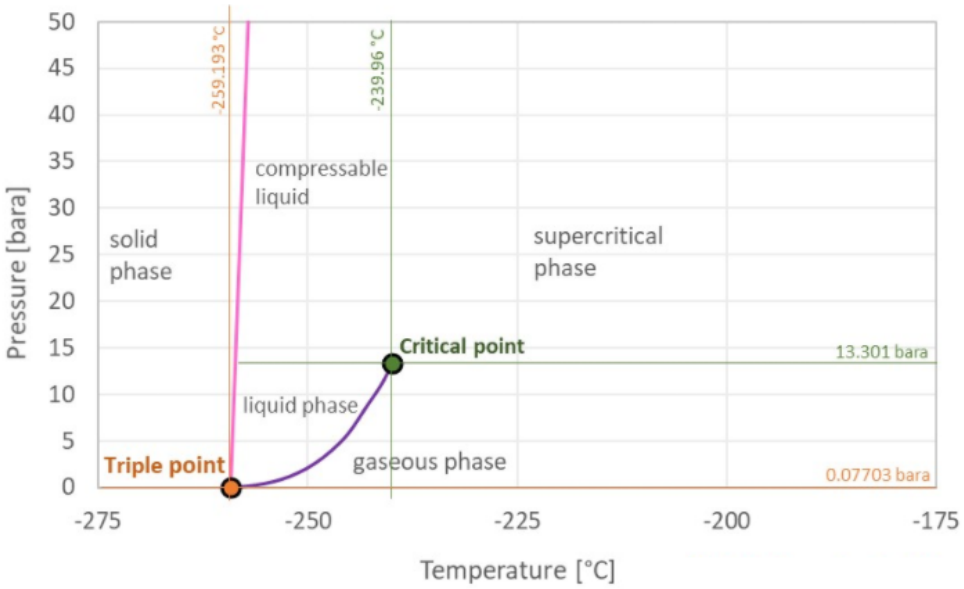

Figure 2.6: Hydrogen phase diagram [11]

Optimal storage pressure and temperature for liquid hydrogen is 1 bar and -253°C. If the temperature was to increase from this point, the hydrogen phase would move to the right in figure 2.6 and cross the boiling point curve (purple curve). At this combination of pressure and temperature, liquid hydrogen will start to boil and transition into gas, in which it will expand about 800 times. This will cause a two-phase flow to be present in the piping system with more complicated flow patterns. The gas-phase transition should be avoided because the process of liquefying hydrogen is expensive in terms of energy and the liquefaction equipment is usually not readily available. Boil-off can, for example, be used to pressurize a tank truck during bunkering to avoid losses.

2.4 Two-phase flow

In applications with liquid hydrogen, it is very common to have a two-phase flow. Some amount of boil-off gas is inevitable in a bunkering system, so a two-phase flow with liquid and gas is very likely to happen. The phase of liquid hydrogen trough a bunkering system will be investigated in this report using FFI's experiments as a basis. A thermodynamic equation of state solver will be used to study when boiling occurs in the pipeline and attempts to provide a bunkering pressure and temperature to minimize losses to boil-off.

Several flow regimes exist within the definition of two-phase flow, such as annular and slug flow. Figure 2.7 shows a flow regime map dependant on mass fluxes of liquid and gas together with sketches of the different flows in a pipe. These figures are based on a water/air mixture in a 5.1 cm horizontal pipe [12].

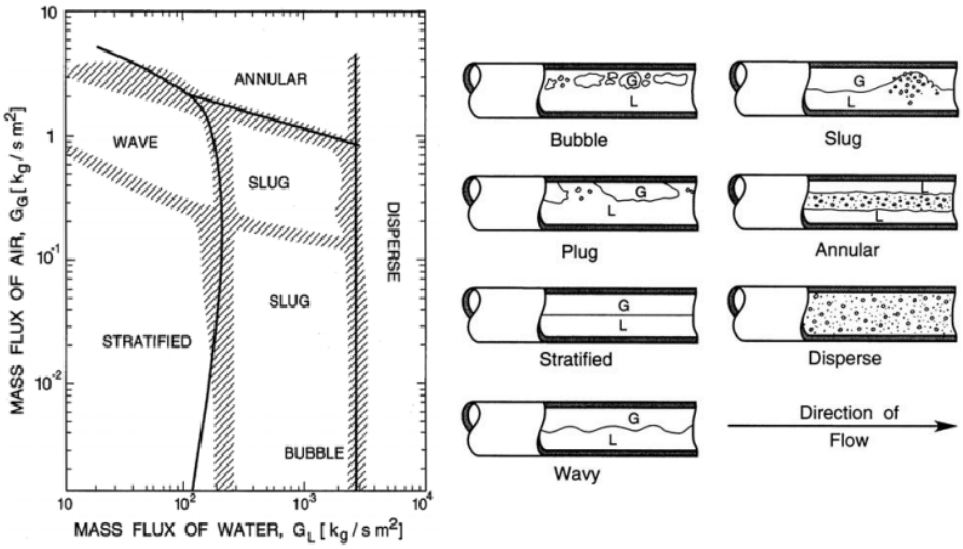

Figure 2.7: *Left*: Flow regime map *Right*: Sketches of flow regimes in pipes [12]

Agarwal R. and Dondapati R. S. investigated numerically liquid hydrogen flow in cryogenic feeding lines in terrestrial- and microgravity conditions [13]. A CFD analysis was conducted to simulate two-phase flow in a vertical insulated pipe fed from the bottom. This study found clear slug flow behavior in terrestrial conditions which is consistent with present flow regime maps. Figure 2.9 shows the resulting flow in terrestrial gravity conditions.

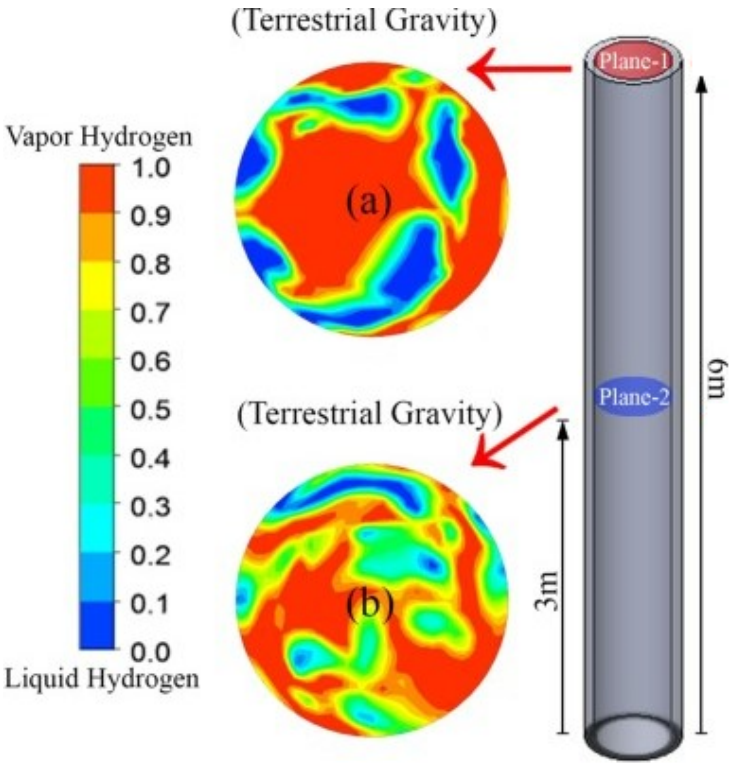

Figure 2.8: Resulting flow in terrestrial gravity from CFD analysis [13]

Slug flow is of great importance in industrial pipe flow, as it can cause pressure fluctuations and large-scale vibrations in a system. This flow regime is a gas/liquid flow characterized as a series of liquid slugs containing dispersed bubbles alternating with larger bubbles [14]. Slug flow can occur over a wide range of mass flows and fluid types. Figure 2.9 shows a typical slug flow in a pipe.

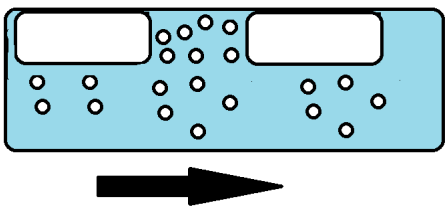

Figure 2.9: Typical slug flow in a horizontal pipe [15]

2.5 Safety challenges

Handling of cryogenic fuels such as LNG and LH2, poses several safety challenges in bunkering. The two fuels are quite similar in terms of safety concerns, but LNG has been used in industry for a long time compared to LH2 and has built up a regulatory framework around the safety aspect in industry. The main hazards when using LNG are fire and explosions, cryogenic freeze burns, embrittlement of equipment material and safety implications linked to confined spaces [16]. This is also true with the use of liquid hydrogen.

2.5.1 Fire and explosions

The most destructive and deadly hazard is explosion and fire. If LH2 were to leak from piping or other equipment, it will rapidly evaporate and create a flammable cloud with the air. Hydrogen has a wide flammability limit, from 4% to 74% in air, as well as a low ignition energy of only 0.02 millijoules, making the cloud very easy to ignite [17]. Fortunately, a bunkering system is commonly located outside, which will mitigate the hazard of a release as there is an abundance of air usually paired with some wind. Hydrogen is also buoyant and will rise and disperse quickly in air. In FFI's experiments, 3 ignited tests were conducted to investigate the safety challenges a leak would pose [10]. In test 6 a typical bunkering mass flow of 49.9 kg/min was used for the release. The highest H_2 concentration 30 meters from the release point was 18.6% to 21.0%, well inside the flammability limits.

2.5.2 Cryogenic burns

Personnel working with cryogenic fluids may be exposed to the liquid or gas during a leak. The cryogenics are extremely cold and can freeze skin and tissue quickly, resulting in a cryogenic burn [18]. It is important to use safety equipment specifically designed for use with cryogenic liquids. Workers should be trained in handling of cryogenics to minimise the risk of any accidents.

2.5.3 Hydrogen embrittlement

Hydrogen embrittlement is the degradation of metal, typically steel, in contact with H_2 or LH2. The embrittlement of the metal will reduce ductility and strength making fractures and failure more likely. Hydrogen will dissolve into the material, initiating changes on a microscopic level [19]. Austenitic stainless steel is less susceptible to embrittlement from hydrogen and is a commonly used material in hydrogen applications [20].

2.5.4 Confined spaces

A release of hydrogen in a confined space during bunkering can happen inside the receiving vessel. The confined space leak poses risks for all personnel currently on the ship, as the explosion hazard is high. The second part of FFI's work on leakage was inside a confined space [10]. The confined space in this experiment had a volume of about $24m^3$, and both unignited and ignited tests were conducted. The results show that within only a few seconds, with the lowest mass flow in test 8, the room is fully saturated with H_2 gas. Initially, this poses mostly a risk of suffocation as the fraction rapidly increases to 100%. This fraction is outside the flammability limit for hydrogen, so the chance of ignition is low during the leak. However, there is a risk that an explosion can occur when the leak is stopped and the fraction of H_2 goes down.

3 Current bunkering technology

This chapter will present different bunkering methods currently used today, generally in applications with LNG. There are several ways to bunker a ship, depending on the fuel type. The most common methods of bunkering cryogenic fuels (LNG and LH2) are ship-to-ship-, shore-to-ship- and truck-to-ship bunkering. This chapter will discuss the advantages and disadvantages of all three systems. A presentation of a bunkering system will be presented with brief explanations of equipment and facilities. This chapter will focus mainly on LNG, as LH2 still is not commonly used as a maritime fuel.

3.1 Bunkering methods

3.1.1 Ship-to-ship

In ship-to-ship bunkering scenarios, the receiving ship will be moored to the bunker ship in preparation for the refueling. A flexible hose controlled by a crane will be used to connect the bunkering line to the receiving ship. It is common to have several checks to make sure there are no leaks or other problems with the hose and connections. The bunkering process is typically driven by a pressure difference from the bunkering tank to the receiving tank. It is also possible to use a pump. Bunkering can take up to an hour depending on the size of the receiving ship. Typical transfer rate is 320 m^3/h [21]. Figure 3.1 shows a ship-to-ship bunkering process.

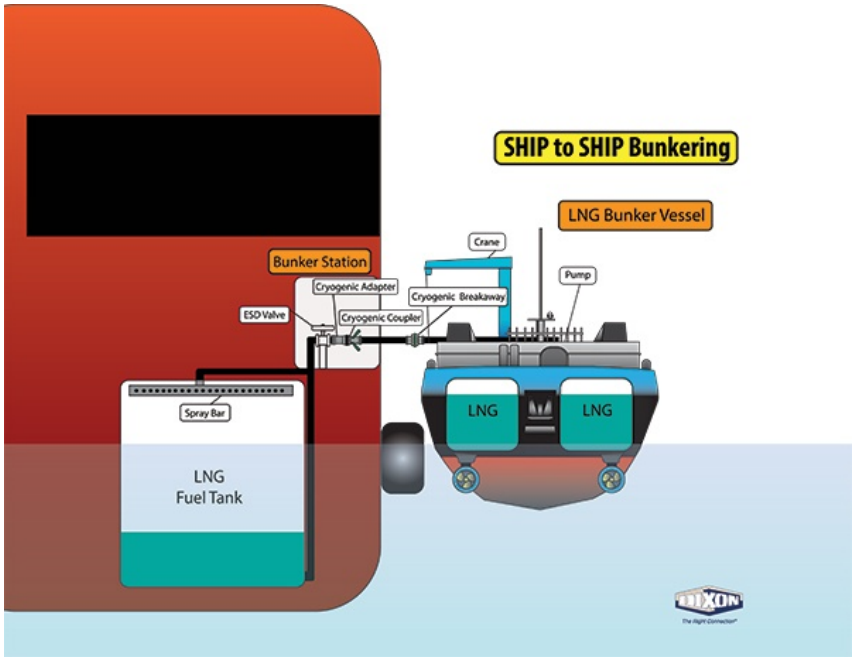

Figure 3.1: Schematic of ship-to-ship bunkering [22]

Advantages

There are several advantages with ship-to-ship bunkering. It is more efficient to bunker a ship outside of port if that ship has no business in said port. The bunkering- and receiving vessel can maintain distance from other ships, making the process safer in terms of a potential leak. A ”movable” fuel station can be practical in many regards. If a long travel distance has few or no ports to refuel, a bunkering vessel can be moved to a key location along the route to ensure sufficient fuel. Furthermore, it allows ships to receive cargo at the same time as bunkering if the port restrictions allow it.

Disadvantages

Using ship-to-ship bunkering also comes with downsides. Successful bunkering depends highly on the weather conditions, as bad weather will complicate the process. Safety is an important aspect when considering LNG ship-to-ship bunkering. To ensure safe bunkering, the crew onboard both ships need special training to handle cryogenic equipment and procedures. Several safety systems need to be installed on both ships, such as emergency shut-down systems, which must be checked before all bunkering procedures. The bunkering vessel needs to be equipped with a gas detection system [23].

3.1.2 Shore-to-ship

Another way to bunker a ship with either LNG or LH2 is shore-to-ship bunkering. Here, the fuel is either directly transferred from a production facility, from an intermediate tank, or to an import/export terminal. The Mongstad industrial park in Norway has port facilities that employ shore-to-ship bunkering from a production plant. There are currently 23 ports with LNG bunkering capabilities in Europe, with more planned and under construction [24]. An LNG bunkering facility can be modified to handle LH2 at a later stage. Figure 3.2 shows a shore-to-ship bunkering process using an LNG storage tank.

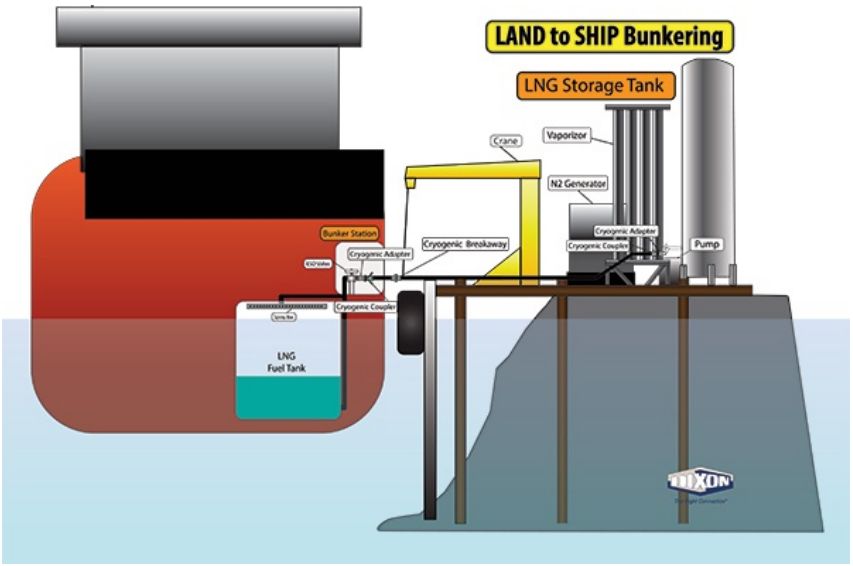

Figure 3.2: Schematic of shore-to-ship bunkering with LNG storage tank [22]

Advantages

It is advantageous to have a terminal-to-ship bunkering facility in ports with high demand. A stable supply of fuel (LNG or LH2) provided by a production plant nearby is a good solution. In this kind of system, the flexible hose and loading arm is fixed to the port, allowing for a larger hose diameter providing higher mass flow and shorter bunkering times [25]. Furthermore, the port providing the bunkering system will have trained personnel to handle the process together with the necessary equipment. This limits the need for personnel trained in the use of cryogenic-equipment onboard the receiving vessel.

Disadvantages

A disadvantage of the shore-to-ship bunkering method is that the terminal is stationary, so the receiving ships must dock to be refueled. This can limit the number of ships able to bunker at certain ports depending on the size of the ship compared to the port. Furthermore, an LNG terminal is typically quite large depending on the port's demand. Not all ports have the required space to build an LNG terminal close by. A steady supply of LNG from a production plant is also required together with a liquefaction plant.

3.1.3 Truck-to-ship

The bunkering method of truck-to-ship is currently the most used method with LNG [25]. The fuel is transferred from a supplying truck to the ship using a flexible hose with a crane. The driving force in the transfer can be either pressure-driven or by using a pump. This is currently the most common way of bunkering LNG due to generally low demand and little investment into the newer ship fuels. Figure 3.3 shows the bunkering process.

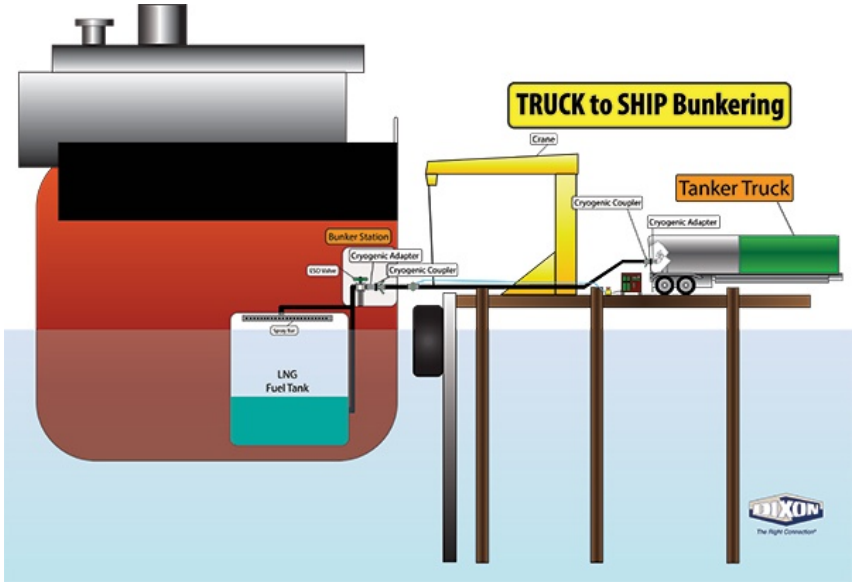

Figure 3.3: Schematic of truck-to-ship bunkering [22]

Advantages

A great advantage of truck-to-ship bunkering is the low investment costs it entails. The LNG or LH2 production facility can be located further away from the port and all ports will be able to receive fuel from trucks. The production plant will also be able to deliver fuel to many ports or terminals at the same time.

Disadvantages

One of the disadvantages of using truck-to-ship bunkering is the limiting factor of truck size. A typical truck can carry between 40- and 80 m^3 of fuel which is only enough for smaller ships. It is also limited by bunkering rate, as a truck bunkers at about 1000 l/m. Moreover, a ship usually can not bunker from a truck and load/unload cargo at the same time. This is disadvantageous if a ship is at the port to unload and fuel before continuing.

3.2 System

A bunkering system consists of several facilities depending on the bunkering method. This chapter will briefly present the required main system components in a bunkering system using cryogenic fuels.

Several facilities are required to have a working cryogenic fuel bunkering system. A supply of raw material, a production plant and transport between the facilities is required. Figure 3.4 shows an LNG production system with a production platform, liquefaction, and ways of transportation.

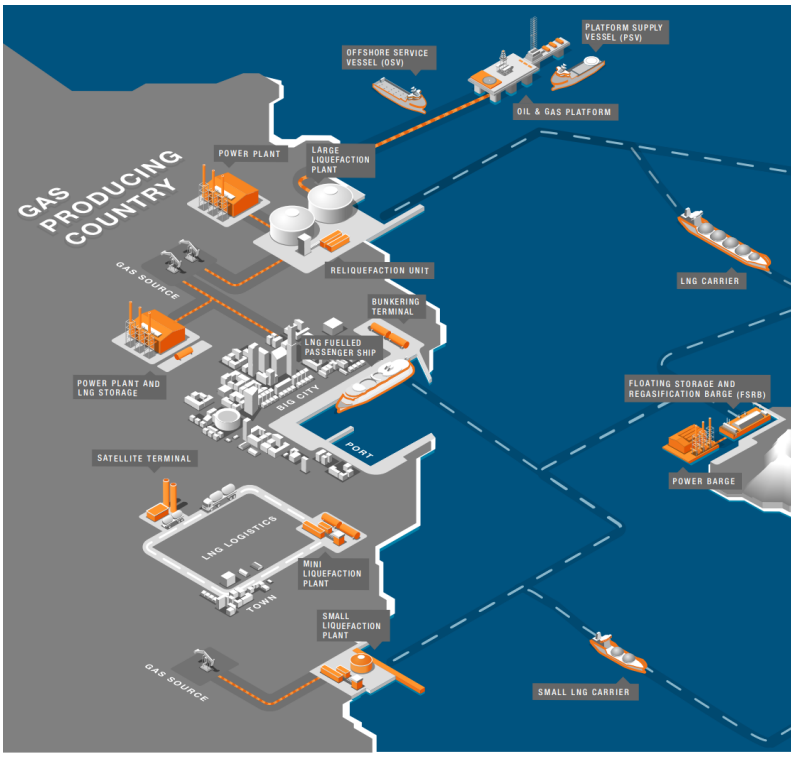

Figure 3.4: LNG bunkering system from Wärtsila [26]

Currently, these kinds of systems are only viable for LNG as there is not enough demand for LH2. In the next decades, as more environmental demands are put on the maritime transport industry, new developments of similar systems with LH2 will emerge. The next section presents the production, liquefaction and main equipment required in a liquid hydrogen system.

3.2.1 Production

Production of LH2 starts with the production of hydrogen gas, usually from steam-methane reforming. Hydrogen gas can be produced from electricity as well, through electrolysis. Electrolysis is considered the "best" alternative in terms of environmental impact.

3.2.2 Liquefaction of hydrogen

Liquefying hydrogen is an energy-expensive process and uses advanced technology to achieve the low temperatures required. Hydrogen liquefies at 20 K (-253° Celsius) at atmospheric pressure using heat exchangers, compressors, and expansion equipment. Hydrogen was first liquefied by Sir James Dewar in Scotland in 1898, using pre-cooled carbolic acid and liquid air to cool pressurized hydrogen gas. This system is similar to the Hampton-Linde cycle used to liquefy air. Several other liquefying processes exist such as the Claude cycle, Collins Process and Helium Brayton Cycle [27].

The simplest way to liquefy hydrogen is the Hampton-Linde cycle, also known as the Joule-Thompson expansion. The cycle uses the Joule-Thompson effect to liquefy the gas, which describes the temperature change of a real gas when it flows through a valve [28]. Hydrogen gas is initially compressed and cooled by a cooler and heat exchanger before undergoing isenthalpic expansion across a valve. By pre-cooling the gas below the inversion point (about -73° Celsius for hydrogen), the gas will be further cooled when expanded.

The complex process of liquefying hydrogen can use between 20 % and 30 % of the energy content using today's technology [29]. There is a great potential in increasing the thermodynamic efficiency in the system as well as cost by reducing total work input to the compression cycle. Costs can be reduced further by using inexpensive sources of electricity, for example gas or steam turbines. Improved insulation technology, advanced thermal management systems, and integration of ortho- and parahydrogen converters, will further reduce cost and increase efficiency. The U.S Department of Education (USDOE) is supporting the development of a new liquefaction plant that will use the combined-reverse-Brayton-Joule-Thompson cycle (CRBJT).

The cycle is based on the Joule-Thompson expansion cycle paired with highly efficient isentropic expansion [30]. Figure 3.5 shows a simplified CRBJT cycle.

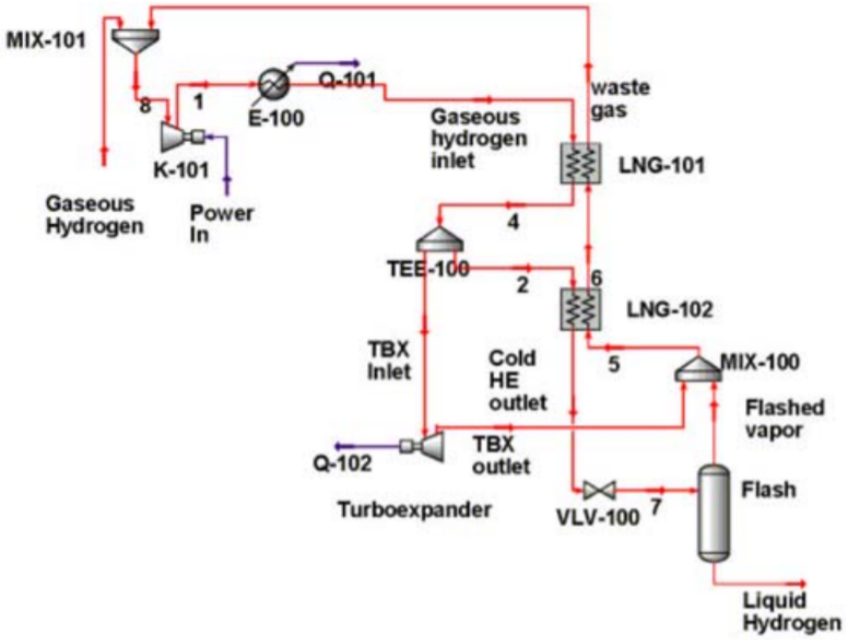

Figure 3.5: Combined-reversed-Brayton-Joule-Thompson cycle [31]

3.2.3 Bunkering equipment

Piping and storage

A bunkering system with cryogenic fuels requires advanced equipment. To avoid losses to boil-off, the thermal conductivity of piping and storage tanks need to be kept at a minimum. This is done by vacuum insulation between the outer and inner walls. The pipes and storage tanks have an outer and an inner wall with a space between them. This space is usually filled with perlite (or an equal material) and a vacuum is applied. This ensures a very low thermal conductivity (0.001 W/mK [32]) and excellent insulation properties.

Crane and flexible hose

The setup for connecting the bunkering hose to receiving vessel consists of a crane and a flexible hose together with coupling equipment. The crane is operated by trained personnel either in port or on the ship. Furthermore, the flexible hose is connected to the ship via a drip-free, breakaway coupling. This coupling ensures no dripping of fuel when disconnecting after bunkering, and the breakaway feature protects against breakage if large movements were to occur [21]. The coupling serves as the weakest part of the connection, breaking off if excessive force is applied.

Safety equipment

Typical bunkering systems are fitted with an emergency release valve which releases the fuel into a separate system leading to a ventilation mast. Releasing the fuel into the air above the ship reduces the chances of any hazards as the gas will disperse quickly in the air.

4 Method

This section presents the different models used in the report. The models are presented separately in this chapter, but tie into each other later in the report.

4.1 Pressure loss model

The pressure loss model aims to verify the use of a standard pressure loss calculation in use with liquid hydrogen flow in pipes. The calculated pressure loss will be compared to the measured pressure in FFI's experiments later in the report. A standard pressure loss calculation using the Darcy-Weisbach equation is presented below. The following assumptions are made:

- Incompressible fluid
- Only liquid phase hydrogen
- Constant pipe diameter
- Using absolute roughness of 316L SS steel: ε=0.015mm

The following section presents the method used for calculating the pressure drop over the pipes [33]. Note that this is only the piping, not including the flexible hose and tanker setup. Table 4.1 contains the definitions of all symbols used in the calculations.

Table 4.1: Symbol explanation

Symbol	Definition
V	Velocity
ΔP	Pressure from friction or minor loss
f_d	Darcy friction factor
Re	Reynolds number
K	Minor loss coefficient
ρ	Density of fluid
ε	Absolute roughness of pipe
L	Length of pipe
D	Diameter
μ	Dynamic viscosity

To calculate the pressure loss in the pipes, the Darcy-Weisbach equation can be used:

$$\Delta P_{major} = \frac{f_D L \rho V^2}{2D} \tag{4.1}$$

In equation 4.1 everything is known except the Darcy friction factor, f_d. The first step is to calculate the Reynold number as in equation 4.2.

$$Re = \frac{\rho V D}{\mu} \tag{4.2}$$

In cases where pressure difference is used to move liquid hydrogen, turbulent conditions are assumed. Furthermore, the Darcy friction factor is calculated using Moody's Colebrook approximation shown in equation 4.3.

$$f_D = 0.0055 \cdot \left[1 + \left(2 \cdot 10^4 \cdot \frac{\varepsilon}{D} + \frac{10^6}{Re} \right)^{\frac{1}{3}} \right] \tag{4.3}$$

Using equations 4.1-4.3, the pressure loss due to friction can be calculated. Furthermore, the minor losses, Δp_{minor}, accounts for the energy lost in pipe fittings, valves, inlet etc. that exists in the piping system and is defined as:

$$\Delta p_{minor} = \sum K \frac{\rho V^2}{2} \tag{4.4}$$

Typical K values are found in fluid mechanical texts. The total pressure loss in the piping system can then be expressed as:

$$\Delta p_{total} = \Delta p_{major} + \Delta p_{minor} = \frac{f_D l \rho V^2}{2D} + \sum K \frac{\rho V^2}{2} \tag{4.5}$$

A Python script is used to calculate the pressure loss.

4.2 Helmholtz EOS

This section presents the thermodynamic model used in this report. The model uses a solver for a Span-Wagner type equation of state and is made by Are Mjaavatten. A brief explanation is given along with the general equations.

The derivation given below is from the work of Are Mjaavatten and is a reproduction of reference [34].

Table 4.2 gives an overview over the symbols used in this section.

Table 4.2: Symbol explanation

Symbol	Definition
F	Helmholtz free energy
U	Internal energy
T, T_s	Absolute temperature, saturated temperature
S	Entropy
V	Volume
N	Array of mole numbers
v	Molar volume (V/N)
g	Thermodynamic state

The EOS solver used in this work is based on Helmholtz free energy, which describes obtainable work in a closed thermodynamic system with constant temperature. Helmholtz free energy is defined as:

$$F \equiv U - TS \tag{4.6}$$

If a fluid system at thermodynamic equilibrium is considered and an assumption is made that the expression for Helmholtz free energy F as a function of temperature T, volume V and the array $\boldsymbol{N}$ of mole numbers of all constituent chemical species is known, function 4.7 is known.

$$F(T, V, \boldsymbol{N}) \tag{4.7}$$

Function 4.7 is a fundamental thermodynamic relationship and it can be shown that this function contains all thermodynamic information about the system. This means that the state is uniquely determined by T, V and $\boldsymbol{N}$ [34]. In this report, a two-phase system is considered with both liquid and gas phase hydrogen. An expression for the saturation pressure as a function of temperature ($p_{sat}(T)$) was presented by Leachman and co-workers in 2009. This expression can be used with the expression for Helmholtz free energy to find the state of saturated vapour and saturated liquid at temperature T_s. Then, equation 4.8 must be solved.

$$g(v) \equiv p(T_s, v) - p_{sat}(T_s) = 0 \tag{4.8}$$

This model can accurately calculate thermodynamic states in liquid hydrogen through a process.

4.2.1 Hydrogen parameters and state definition

Several parameters used in the other models are obtained from the Helmholtz solver in MATLAB, such as liquid- and gas fractions, heat capacity and density. A bunkering system is programmed in a script using FFI's tests as foundation. Firstly, the desired fluid is selected by defining a thermodynamic object, in this case as H_2. Secondly, the thermodynamic properties are defined together with the state of saturated liquid and initial temperature. Thirdly, the state of the tank is defined with the initial pressure from FFI's experiments depending on which test is currently considered. Finally, the system undergoes an isenthalpic process using data from FFI as reference pressure at each sensor. The thermodynamic state at every sensor is then defined and from here, all parameters can be calculated.

4.2.2 Hydrogen phase in the system

The Helmholtz EOS solver is also used to investigate the phase of the fluid through the system. The phase is given by a constant enthalpy process (friction) which is plotted in a P-V diagram with the saturation curve. The first test in FFI's experiment is used as reference as it is not pressurized by an auxiliary system and the liquid is saturated. An initial saturation temperature is set to 24.45 K and the following saturation pressure is compared, and should be equal to, the tank pressure in test 1. Furthermore, the pressure is varied to see how the initial tank pressure affect the phase of the fluid through the system.

4.3 Mass flow model

In the work done by FFI, the given mass flows are calculated using the "LINEST" function in Microsoft Excel to fit the mass data. This function uses the "least square method" to calculate a straight line on the form $y = mx + b$ that best fits the data provided [35].

In this work, an attempt to improve the mass flow model is done with a second degree polynomial instead of a straight line to better fit the mass data. A polynomial of the form $y = ax^2 + bx + c$ is used to fit data gathered in FFI's experiments. The mass flow is obtained by mathematical derivation of the equations in each test. Deriving the expressions, $y' = 2ax + b$ and $y' = m$, yields the mass flows of the fitted data. The straight line gives a constant mass flow while the polynomial will have a mass flow that varies with time.

The mass flow from the polynomial is used in the pressure loss calculations to calculate velocity in the Darcy-Weisbach equation. The *polyfit* function in the numpy library in Python was used to make the second order polynomial function.

4.4 Model for nozzle mass flow

This section describes the use of, and the derivation of the Clausius-Clapyron equation used to calculate the mass flow rate out of the nozzle. The full mathematical derivation can be found in reference [36].

The Clausius-Clapyron equation is used in the calculation and shown below.

$$Q_m = \frac{\Delta H_v A}{v_{fg}} \sqrt{\frac{g_c}{TC_p}} \tag{4.9}$$

Table 4.3 gives an overview of all the symbols used in the following derivation.

Table 4.3: Symbol explanation

Symbol	Definition
Q_m	Mass flow
ΔH_v	Heat of vaporization
A	Area
v_{fg}	Difference in specific volume between vapor and liquid
g_c	Unit converter (equal to 1 for SI units)
T	Temperature
C_p	Heat capacity
P	Pressure
u	Velocity
v	Specific volume
G	Mass velocity
v_f	Specific volume of liquid
f_v	Mass fraction of vapor
ρ	Density

Equation 4.9 is valid for liquids stored at saturation vapour pressure, $P = P^{sat}$. In this work, the nozzle exit is modeled as a "leak", assuming that kinetic energy dominates the flow and potential energy is negligible.

From a mechanical energy balance, the following can be written:

$$-\int_1^2 vdP = \frac{\overline{u}_2^2}{2g_c} \tag{4.10}$$

Introducing a mass velocity G as $G = \rho\overline{u} = \frac{\overline{u}}{v}$ and combining with equation 4.10 results in:

$$-\int_1^2 vdP = \frac{\overline{u}_2^2}{2g_c} = \frac{G^2 v_2^2}{2g_c} \tag{4.11}$$

Furthermore, solving for mass velocity G and assuming point 2 can be defined at any point along the flow path, equation 4.12 is obtained.

$$G = \frac{\sqrt{-2g_c \int vdP}}{v} \tag{4.12}$$

This equation contains a maximum where choked flow occurs ($dG/dP = 0$). Differentiating and setting equal to zero gives:

$$\frac{dG}{dP} = 0 = -\frac{(dv/dP)}{v^2}\sqrt{-2g_c\int vdP} - \frac{g_c}{\sqrt{-2g_c\int vdP}} \tag{4.13}$$

$$0 = -\frac{G(dv/dP)}{v} - \frac{g_c}{vG} \tag{4.14}$$

Solving for G gives:

$$G = \frac{Q_m}{A} = \sqrt{-\frac{g_c}{(dv/dP)}} \tag{4.15}$$

Given the two-phase flow regime existing in the nozzle, a two-phase definition is required. The two-phase specific volume is given as $v = v_{fg}f_v + v_f$, where v_{fg} is the difference in specific volume between vapor and liquid, v_f is the liquid specific volume and f_v is the mass fraction of vapor. Differentiating this equation for pressure gives:

$$\frac{dv}{dP} = v_{fg}\frac{df_v}{dP} \tag{4.16}$$

Futhermore:

$$df_v = -\frac{C_p}{\Delta H_v}dT \tag{4.17}$$

and

$$\frac{dP}{dT} = \frac{\Delta H_v}{Tv_{fg}} \tag{4.18}$$

Substitution equation 4.17 and 4.18 into 4.16 gives:

$$\frac{dv}{dP} = -\frac{v_{fg}^2}{\Delta H_v^2}TC_p \tag{4.19}$$

Mass flow rate is then determined by combining equation 4.15 with 4.19 which gives the Clausius-Clapyron equation 4.9. The mass flow obtained from 4.9 will be compared to the mass flow given from the tests investigated.

5 Results

This chapter presents the results from the model work. The first section gives a brief analysis of the pressure and temperature in the considered experiments from FFI. The next section contains the results from the attempt to improve the data fitting method from FFI. The findings are summarized in table 5.1. The third section presents the calculation of pressure loss in the system. Here, the measured pressure in tests 1-4 is compared to the calculated pressure using the model presented in section 5.3. A summery of the findings can be found in table 5.2. The fourth section compares mass flow data to a calculated mass flow out of the nozzle, while the final section presents a phase analysis of the liquid hydrogen inside the pipes using FFI's experiments as basis.

5.1 Analysis of FFI's experiments

5.1.1 System pressure

The pressure during the experiment is a key parameter in terms of a bunkering scenario. A plot of the filtered pressure data from FFI's experiments is presented in Figure 5.1.

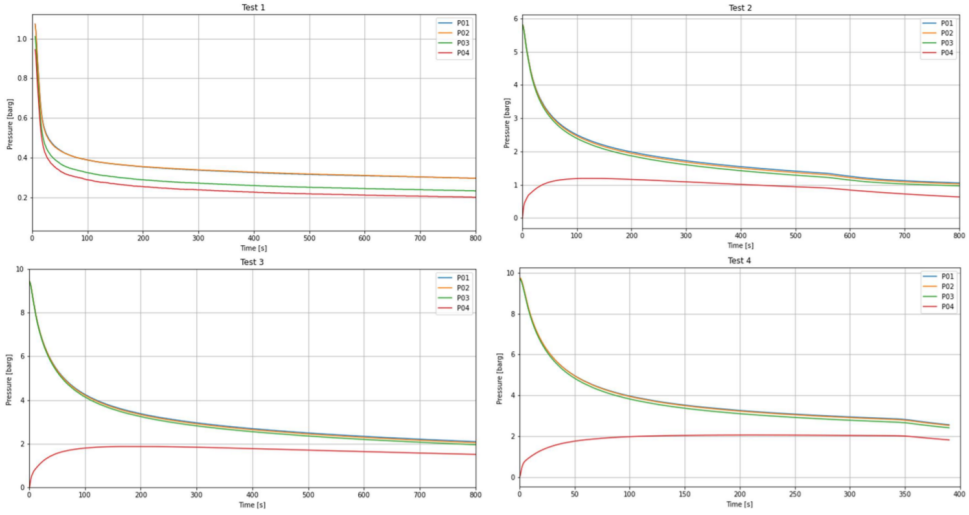

Figure 5.1: Filtered pressure development from Test 1-4

As seen in figure 5.1, the pressure does not change dramatically over the system. The most drastic change is at the beginning, where the flexible hose and tank truck are located. All the tests in figure 5.1 display the same trend: a high pressure drop at the beginning followed by a close-to linear decline during the rest of the experiment. Pressure sensor 4 (red line) is very close to the end valve in the system and shows strange values in the beginning. This is considered to be measurement errors. The total pressure loss during the experiment is found by subtracting data from pressure sensor 1 with data from pressure sensor 4: $\Delta P = P01 - P04$.

5.1.2 System temperature

Temperature change throughout the experiment is an important parameter. In figure 5.2, the filtered temperature data from tests 1-4 are shown.

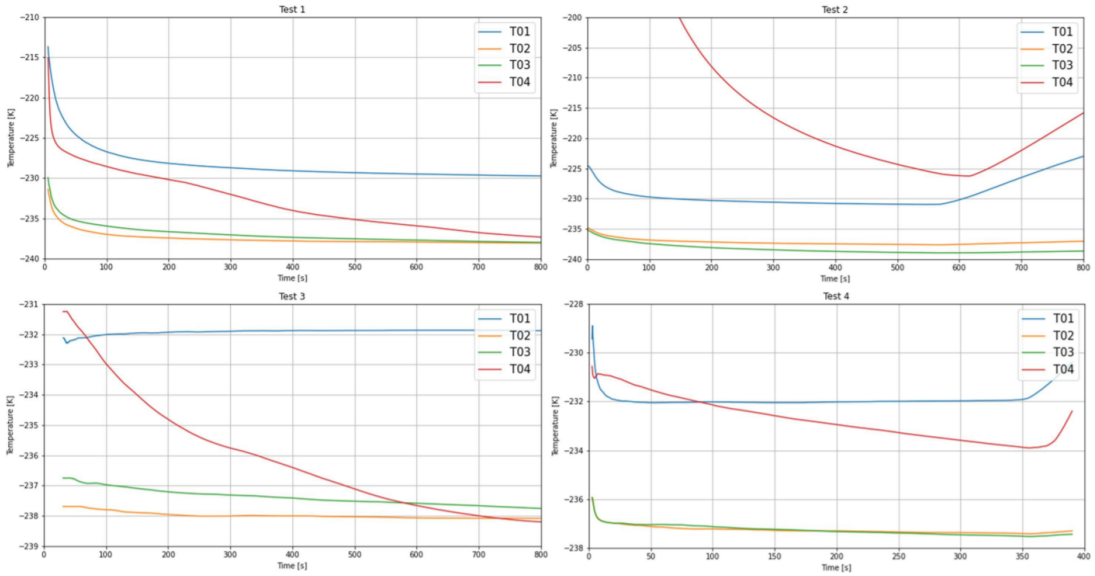

Figure 5.2: Filtered temperature development from Test 1-4

For comparison, the Helmholtz free energy EOS MATLAB model is used to calculate the temperatures at each sensor. From this calculation, the temperature tends towards the same trend as sensors 2 and 3, with a constant temperature of around 24 K (-249°C). Sensors 1 and 4 display a different behavior. In the case of sensor 1, it sits right after the hose connection in the experiment where the pressure drop is large. This creates a possibility of measurement errors. Sensor 4 is located 300 mm before the exit release nozzle where the pressure is ambient. This can also be a source of measurement error.

The temperature sensor and measuring system used in the experiment did not perform as expected during the tests, showing a 10°C higher temperature. The authors of the FFI

report did no further analysis on the validity of the temperature measurements below -200°C. Figure 5.3 displays filtered temperature readings from sensors 1-3, with the 10°C increase, together with the bubble point curve for hydrogen.

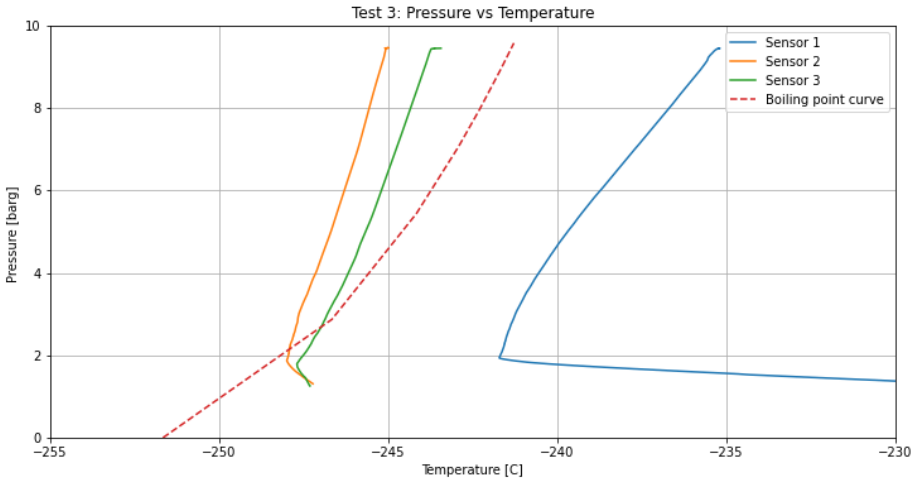

Figure 5.3: Pressure vs temperature plot with bubble point curve using data from test 3

As seen in figure 5.3, sensor 1 displays strange values and is not believed to display representative temperature readings. Sensor 2 and 3 are above the bubble point curve from pressures of 2 barg and upwards. The readings from sensors 2 and 3 trend towards a one-phase flow through the piping system.

5.2 Mass flow

This section presents a comparison of FFI's data fitting, using the least square method with a straight line, and the improved data fitting using the second degree polynomial. Figure 5.4 shows how the straight line fits the mass data while figure 5.5 shows how the polynomial fits to the data.

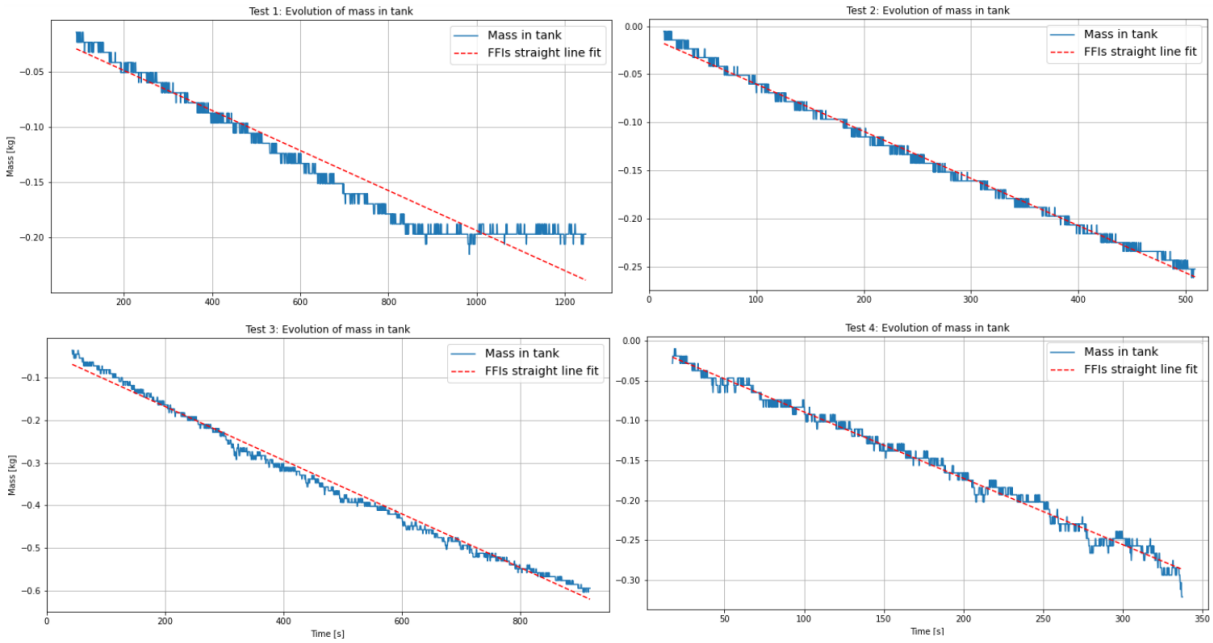

Figure 5.4: Straight line fit using the least square method for tests 1-4

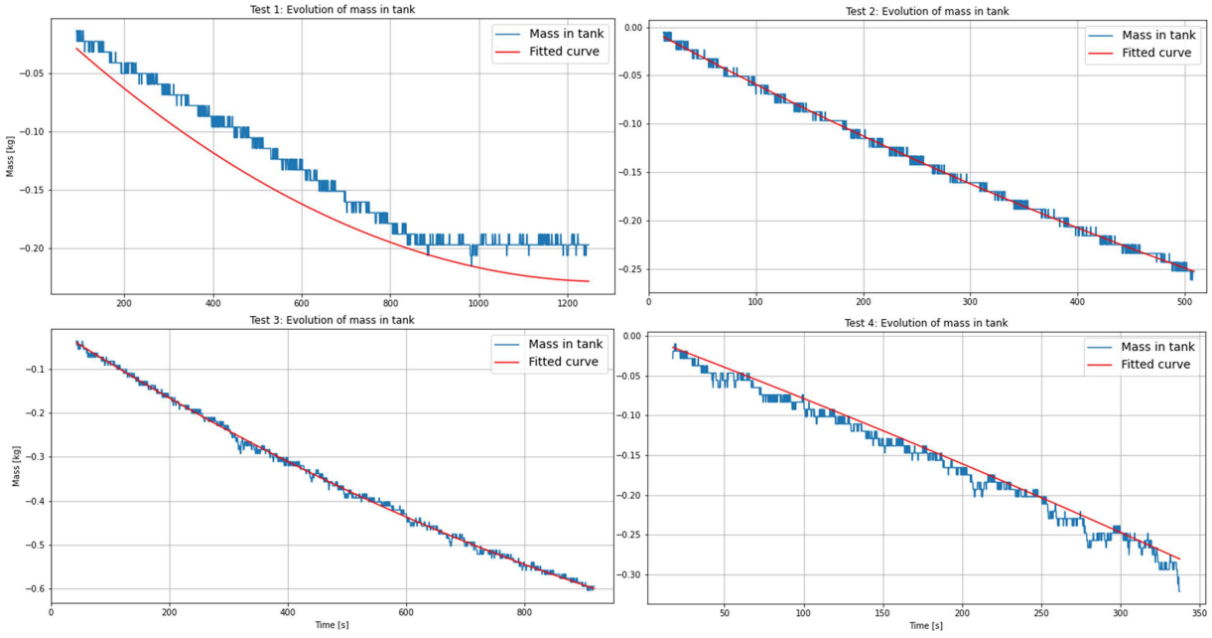

Figure 5.5: Second degree polynomial using the numpy.polyfit function for tests 1-4

As seen in figures 5.4 and 5.5, the accuracy of the methods vary with each of the tests. In test 1, none of the methods display a perfect fit, but the straight line shows a slightly better fit than the polynomial. This is also true for test 4. In tests 2 and 3 the polynomial fits the data better than the straight line.

Using a second degree polynomial to fit the data from the experiments gives a, overall, equal or better fit than the least square method.

Table 5.1 shows a comparison of the calculated mass flow using the least square method and the second degree polynomial. Mass flows derived from the polynomial are calculated with $x = 1$ (the first second) using the derived equation in section 4.3.

Table 5.1: Comparison of mass flows using the least square method and the mathematically derived polynomial

Test nr.	Mass flow using least square method [kg/s]	Mass flows using derived polynomial [kg/s]
1	0.228	0.356
2	0.473	0.592
3	0.630	0.857
4	0.835	0.753

5.3 Pressure loss calculation

Using the method presented in section 4.1 the pressure loss in the system is calculated and compared to FFI's measurements. The model is used to calculate a pressure loss over the piping system with a constant- and a varying mass flow. Sensor $P04$ is not included as it sits right before the nozzle with no insulation, which can affect the measured pressure. The measured pressure loss varies in the tests, but the loss from sensor $P01$ to $P03$ is generally between 5- and 40 kilo pascal (kPa) in all the tests. All calculations uses a K-factor of 1 which accounts for the bend between sensors 2 and 3.

For comparison, a script was made that plots the difference between the measured data from $P01$ and $P03$, the calculated pressure using constant mass flow and the calculated pressure using a varying mass flow. The varying mass flow comes from the derived second-degree polynomial from 4.3 with mass data from FFI. Figure 5.6 shows the plots from test 3.

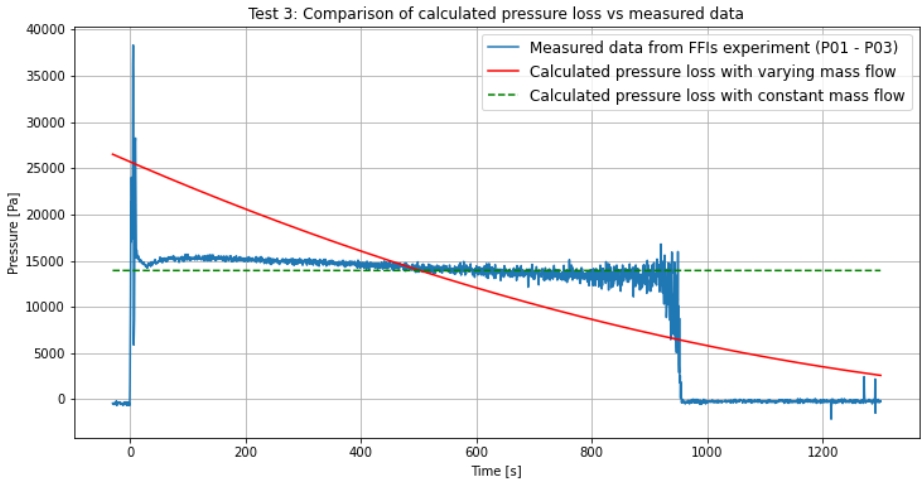

Figure 5.6: Plot comparing measured pressure loss data with calculated values in test 3

As shown in figure 5.6, the estimated pressure loss with the Darcy-Weisbach equation does match quite good with the pressure readings from the experiment. This calculation is only for the piping system, not including the flexible hose and tank truck. Figure 5.6 is plotted from the beginning of the experiment, including the large pressure loss. The varying mass flow calculation has a steep decline with high pressure loss at the start when the mass flow is at its highest. The calculated pressure loss with constant mass flow (green linear line) is very close to the data after the initial pressure loss.

The comparison plots for tests 1, 2 and 4 are shown below in figure 5.7, 5.8 and 5.9, respectively. The figures display the measured mass data from FFI, the calculated pressure loss with varying mass flow and the pressure loss calculated with constant mass flow. For the calculated pressure loss with varying mass flow (red line in the plots), the values referred to in the text is the average value.

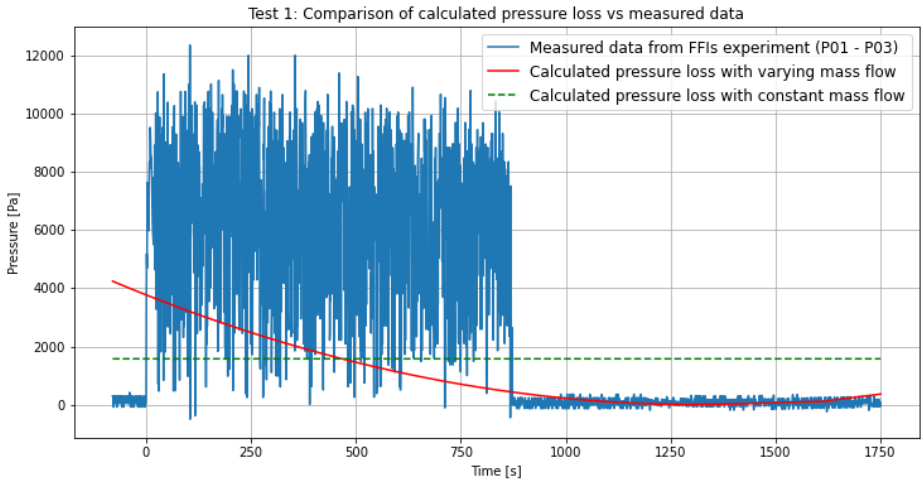

Figure 5.7: Plot comparing measured pressure loss data with calculated values in test 1

The measured pressure in test 1 varies largely between 1 and 11 kPa during the experiment. The calculated pressure is underestimated with 2.72 kPa with the constant mass flow, and between 1 and 3 kPa with varying mass flow.

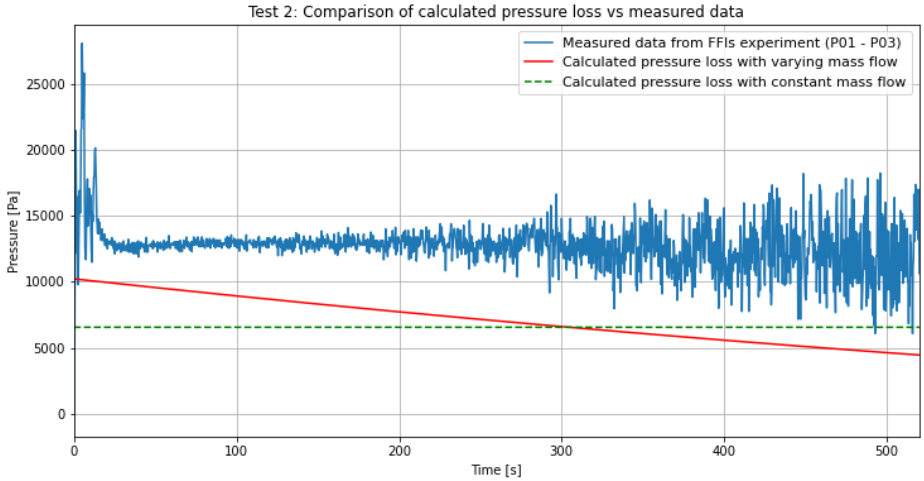

Figure 5.8: Plot comparing measured pressure loss data with calculated values in test 2

Test 2 has a measured pressure loss of 13-15 kPa. Also here, as in test 1, the calculated pressure is underestimated with calculated pressure loss of 6.5 kPa with constant mass flow, and between 4 and 9.5 kPa with varying mass flow.

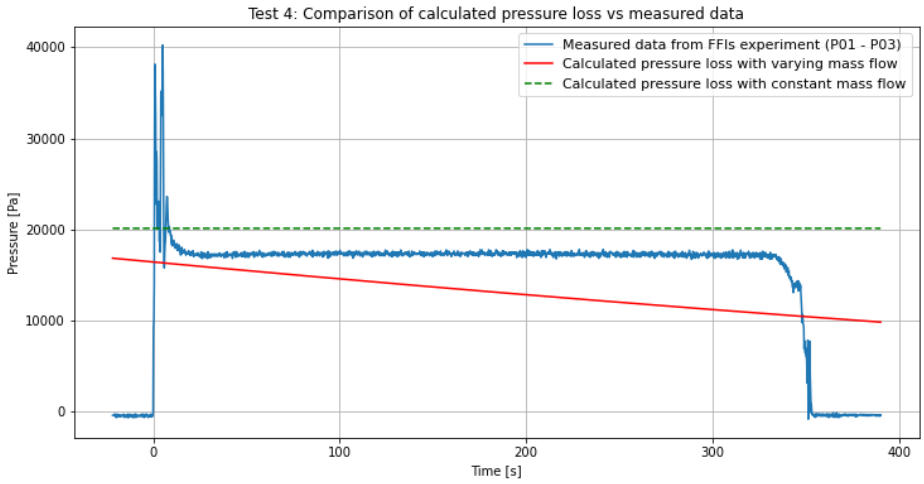

Figure 5.9: Plot comparing measured pressure loss data with calculated values in test 4

In test 4, the calculated pressure with constant mass flow is overestimated, while the calculation with varying mass flow is underestimated. The measured pressure loss is consistently between 15-17 kPa with a peak at the start, while calculated pressures are 20 kPa and 10-15 kPa for constant- and varying mass flow, respectively.

Table 5.2 summarizes the pressure loss findings. To more easily compare the data, an average has been taken over the measured data in the first column, and the calculated data with varying mass flow in the third column. All units are in kPa.

Table 5.2: Summary of the pressure loss findings [kPa]

Test nr.	Measured data	Constant mass flow	Varying mass flow
1	4.29	1.57	1.15
2	7.95	6.55	5.97
3	14.3	8.96	11.3
4	14.6	20.1	13.2

Using the Darcy-Weisbach equation calculates values quite close to the measured data, but is most accurate at higher pressures.

5.4 End nozzle analysis

Using the method presented in section 4.4, a mass flow (MF) out of the nozzle can be calculated and compared to the MF's provided in FFI's experiments. Table 5.3 shows the MF's provided in each test, the MF rates derived from the polynomial and the calculated MF's using the Clausius-Clapyron equation.

Table 5.3: Comparison of provided mass flow from experiments, new mass flow using derived polynomial and calculated mass flow using Clausius Clapyron equation

Test nr.	Provided experiment mass flows [kg/s]	Mass flows using derived polynomial [kg/s]	Calculated mass flow [kg/s]
1	0.228	0.356	1.335
2	0.473	0.592	1.428
3	0.630	0.857	1.518
4	0.835	0.753	1.525

The equation used to calculate the MF out of the nozzle, is an ideal equation and does not take loss parameters, such as friction, into account. While friction over the nozzle is negligible, a discharge coefficient is common to incorporate in the equation, taking the *vena contracta* phenomenon into account. This phenomenon reduces the effective area trough the nozzle which, in turn, reduces the MF. A typical discharge coefficient in an orifice is 0.6. Multiplying the calculated MF's with the discharge coefficient will then give the "real" MF rate. In table 5.4, the calculated MF's is exchanged with the "real" MF's.

Table 5.4: Same as table 5.3 but with calculated "real" mass flow

Test nr.	Provided experiment mass flows [kg/s]	Mass flows using derived polynomial [kg/s]	Calculated "real" mass flow [kg/s]
1	0.228	0.356	0.801
2	0.473	0.592	0.856
3	0.630	0.857	0.911
4	0.835	0.753	0.915

When comparing the "real" MF rates in table 5.4, they are close to the provided MF's, and even closer to the MF's from the derived polynomial at higher experiment MF's. At lower MF's, such as in tests 1 and 2, the calculated MF's are overestimated. The MF's achieved using the derived polynomial are higher than the provided rates from the experiments, and closer to the "real" MF's calculated.

5.5 Phase analysis

Based on the process described in section 4.2.2, the phase of the hydrogen through the system can be analyzed in more detail. Figure 5.10 shows a pressure vs specific volume (V/N) diagram for test 1. Hydrogen will be in a liquid phase above the saturation curve, which is the yellow line, and in the gas phase below it. The blue line is the isenthalp for the process. The following section presents the same P-V diagrams for the remaining tests.

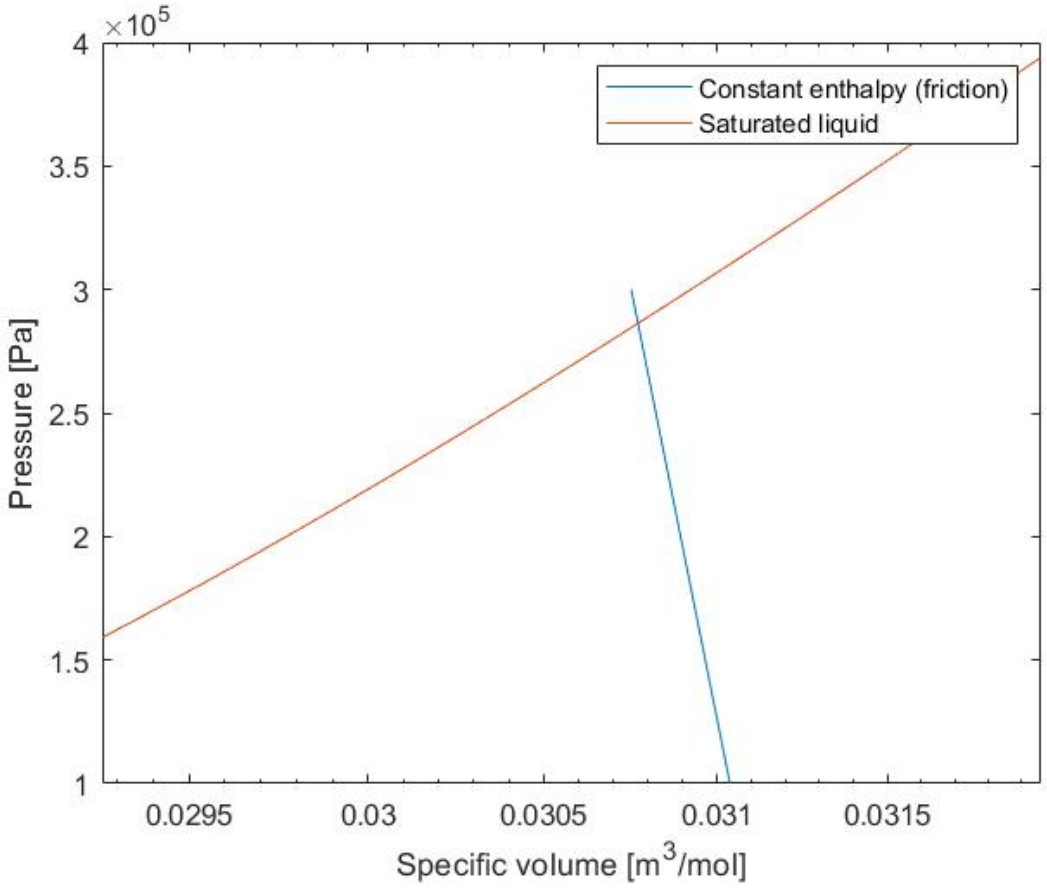

Figure 5.10: P-V diagram for test 1

Figure 5.10 shows the plot for test 1. Test 1 has not been pressurized beforehand and holds a pressure of 3 bar. As the experiment begins, liquid hydrogen will start to boil almost immediately as it passes the saturation curve at 2.8 bar. The boiling will continue throughout the experiment. The specific volume will increase by a small amount during the process.

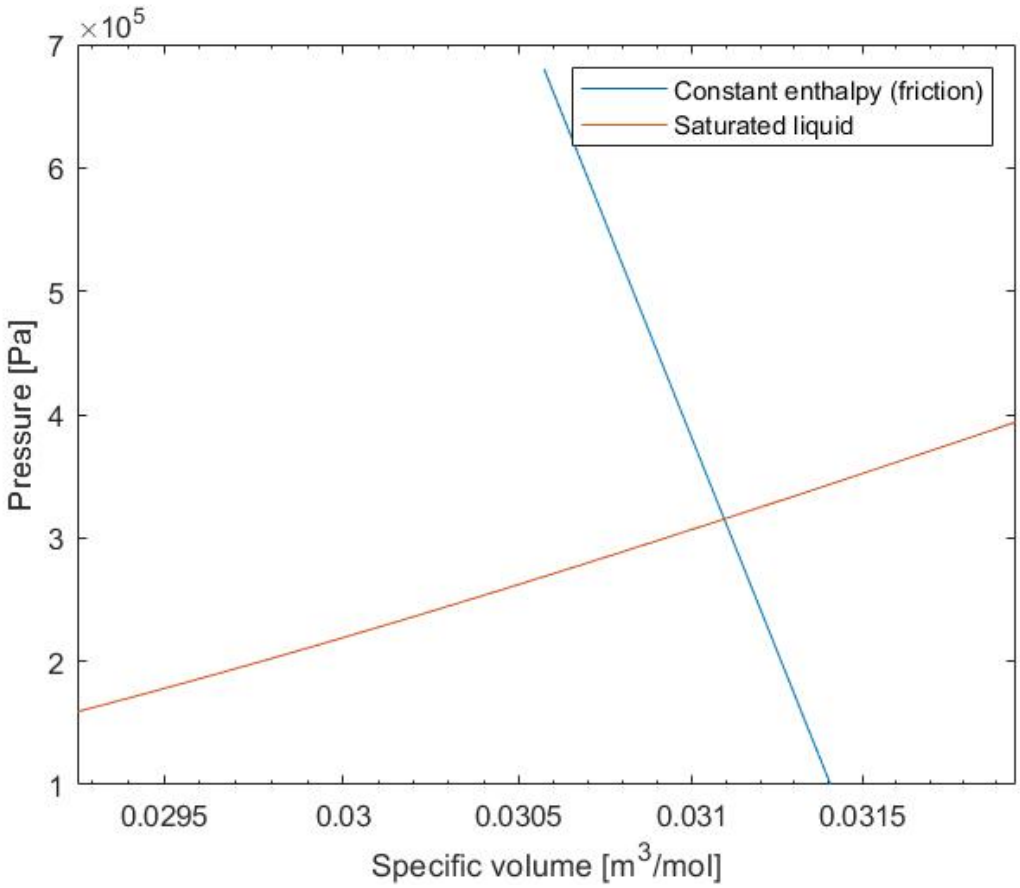

Figure 5.11: P-V diagram for test 2

Plots for test 2 are shown in figure 5.11. Test 2 is pressurized to 6.8 bar before the experiment starts. Here, the liquid will boil later than test 1, but still within seconds after the start of the experiment. The pressure will reach the saturation curve after 3-4 seconds were the liquid will start to boil. In this test, the specific volume increases from 0.0306 to 0.0314 m^3/mol.

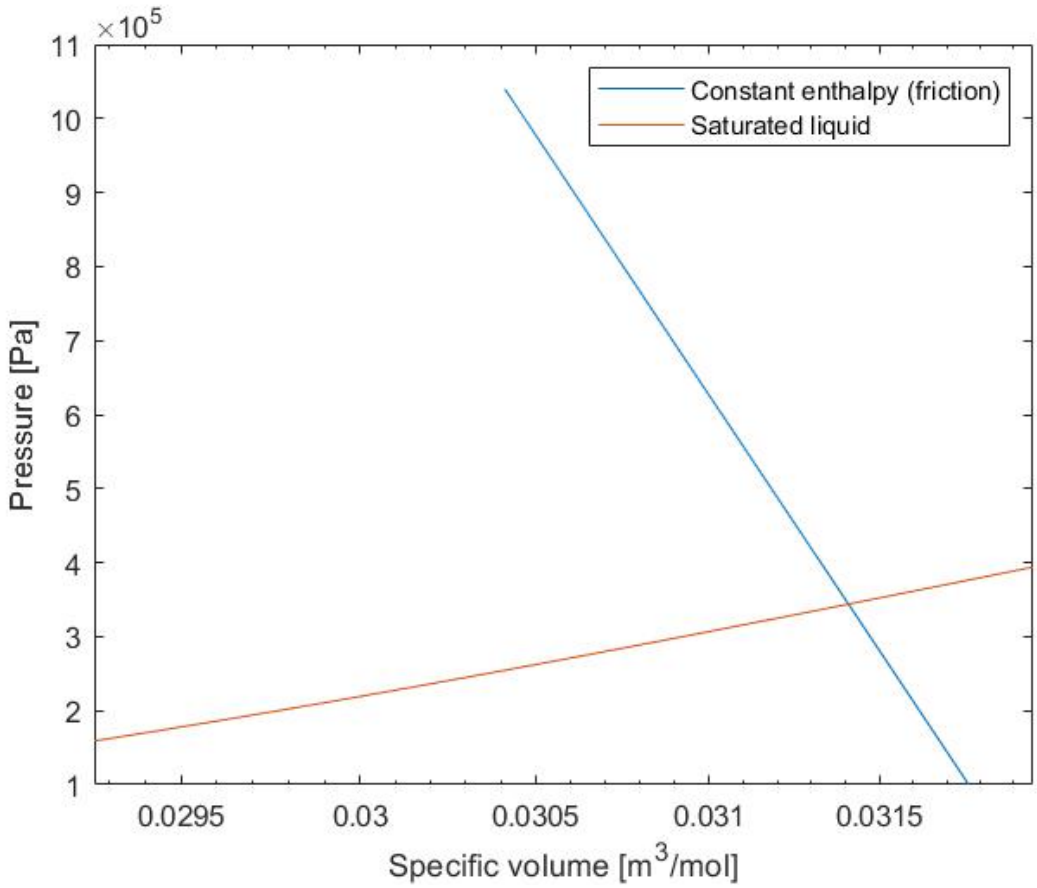

Figure 5.12: P-V diagram for test 3

In test 3, figure 5.12, the boiling will start at a higher pressure, around 3.5 bar. Test 3 is pressurized to 10.4 bar before the experiment begins. It takes 8-9 seconds from the start of the experiment till the pressure drops to, and crosses the saturation curve. The volume increases from 0.0304 to 0.03175 m^3/mol in this test.

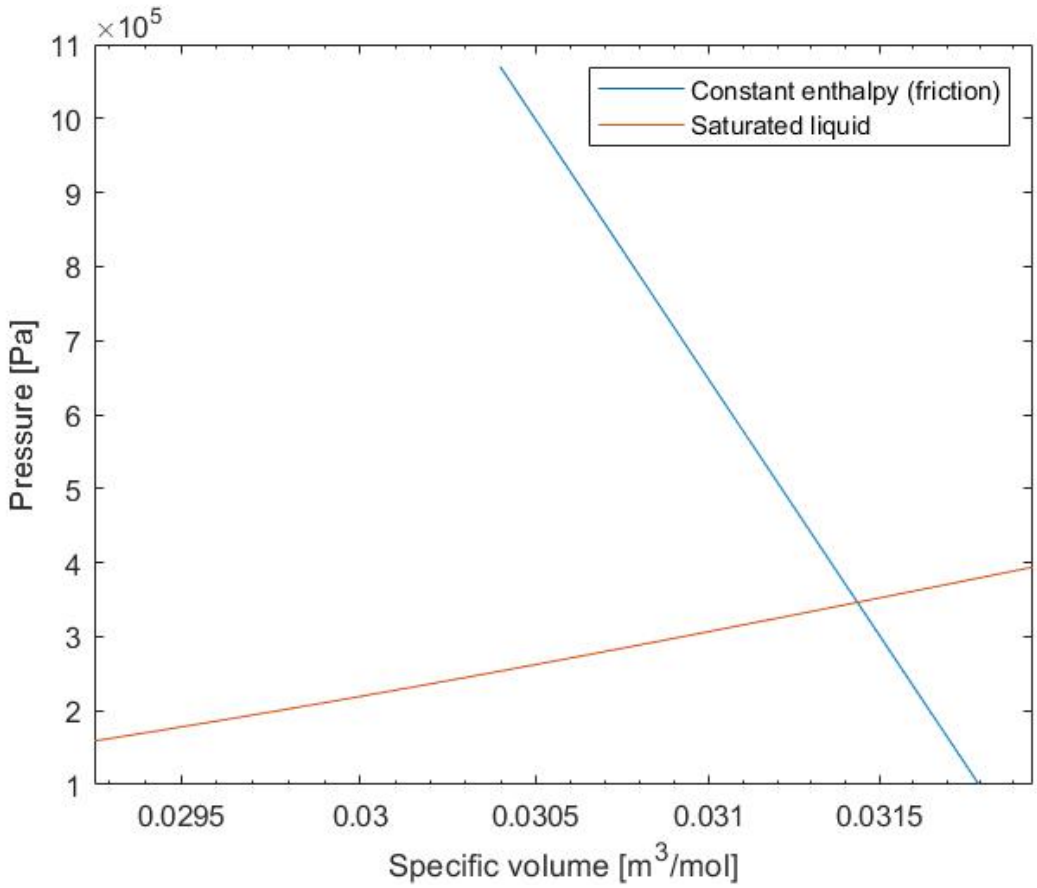

Figure 5.13: P-V diagram for test 4

Figure 5.13 shows the isenthalp and saturation curve for test 4. In this test, the tank is pressurized to 10.7 bar before starting the experiment. The isenthalp will cross the saturation curve at 3.5 bar as in test 3, and it takes 4-5 seconds. The volume increase is about the same as in test 3. Tests 3 and 4 has close to the same initial tank pressure, but test 4 starts to boil in half the time. This is most likely due to the higher mass flow in test 4 (49.7 kg/min) versus the lower mass flow in test 3 of 43.8 kg/min. See table 2.1 for more details on the 4 tests considered.

The results presented in this section shows that the liquid hydrogen in a bunkering system will start to boil early on. The resulting two-phase flow can be damaging to the bunkering system if the flow evolves into a slug flow, for example. This can cause large scale vibrations in the system and pressure fluctuations. During bunkering, the pipe direction is mostly horizontal but can be vertical in the crane setup. As investigated by Agarwal R. and Dondapati R. S. this causes a slug flow in the vertical pipe.

6 Discussion

6.1 Model validity

This section will discuss the validity of the models used in this report and the authors thoughts as to why they are valid/not valid in this work.

6.1.1 Pressure loss model

Constant density assumption

When using the Darcy-Weisbach equation to calculate pressure loss, one assumes that the liquid is incompressible (constant density). In use with liquid hydrogen, it is not proven in the literature that this assumption is valid. Factors such as changes in pressure and temperature and boil-off may lead to a two-phase flow where density change can occur. To check the validity of this assumption the MATLAB script is used to calculate the density of the fluid through the pipe using data from the pressure sensors in FFI's experiment. The calculations show a reduction in density of between 3-4%. This reduction is small, so the assumption is considered valid in this case.

Single-phase flow assumption

In section 5.5 it is established that the liquid hydrogen will boil within seconds of the experiments starting. This causes a two-phase flow in the pipe which the Darcy-Weisbach equation is not suited for. However, the temperature is kept low throughout the experiments so the boiling will be quite slow through the pipeline. Because of the low evaporation rate, the assumption is considered valid within this system. It would be interesting to compare the Darcy-Weisbach equation to a more suitable two-phase flow calculation method, such as the Lockhart-Martinelli method in use with liquid hydrogen.

6.1.2 Helmholtz EOS

Span-Wagner equation of state solvers has often been used in applications with CO_2, with good results. Application to hydrogen with the currently available data seems to give acceptable results as well. The model is only as good as the data provided, which will evolve and improve as more research is done. The Helmholtz EOS used in this work uses data from NIST [37].

6.1.3 Mass flow- and nozzle model

The given mass flow from the experiments is the flow rate out of the tank and not out of the nozzle. In an ideal, incompressible, single phase system the mass flow out of the tank should be equal to the mass flow in the nozzle. This makes the calculated values from the Clausius-Clapyron equation not directly comparable to the mass flows given in the experiments. Despite this, the values at higher pressures are quite close to the experimental data, and even closer to the data derived from the polynomial.

6.2 Hydrogen phase discussion

The plots in section 5.5 shows that it takes longer to cross the saturation curve with an increased pressure. Temperature is also an important aspect of the graph, as it increases the time it takes before boiling occurs. A general advice is to keep the temperature as low as possible, while the pressure should be kept around 10 to 14 bar. This ensures low boil-off and acceptable mass flows in a bunkering system.

6.3 Aspects of a bunkering scenario

This section will attempt to give an overview of a bunkering scenario with current technology and knowledge of the parameters and aspects that are important to consider. A discussion of the tank truck is also included.

6.3.1 Production

Ideally, liquid hydrogen should be produced in the most energy-efficient and environmentally friendly way possible. Using electrolysis is the ”cleanest” option as long as the electricity used comes from low-carbon sources. Liquefaction is an energy extensive process and should be improved upon to further increase its efficiency.

As these technologies are investigated further and improved, steam-methane reforming will most likely still fill the production segment for some years.

6.3.2 Bunkering method

Of the three bunkering methods presented in chapter 3, truck-to-ship bunkering is the most versatile despite the downsides. The technology is readily available, trucks have easy access to remote locations along the shore and there are already existing truck drivers that can transport liquid hydrogen. However, for larger ports with a high demand, the terminal-to-ship method would be recommended.

6.3.3 Bunkering system

Generally, the bunkering system must consist of a bunker vessel, a receiving vessel, and a connecting system. The connecting system needs to have a very low thermal conductivity to avoid losses to boiling. The most frequent technology for this is vacuum-insulated piping. Furthermore, the bunker vessel needs to have a pressure build-up system to allow flow through the piping. All equipment in use with liquid hydrogen must be purged and pre-cooled before any bunkering operations.

6.3.4 Pressure loss in tanker

The biggest pressure loss in the system used by FFI is between the tank and pressure sensor 1. The flexible hose is made of roughly the same material as the piping system, so the loss in pressure could be due to the tank truck. Before the liquid hydrogen can exit through the valve to the flexible hose, it passes several components and a bend. Additionally, the pipe diameter changes from 40 mm to 50 mm inside. Figure 6.1 shows the flow diagram of the tank used in FFI's experiments.

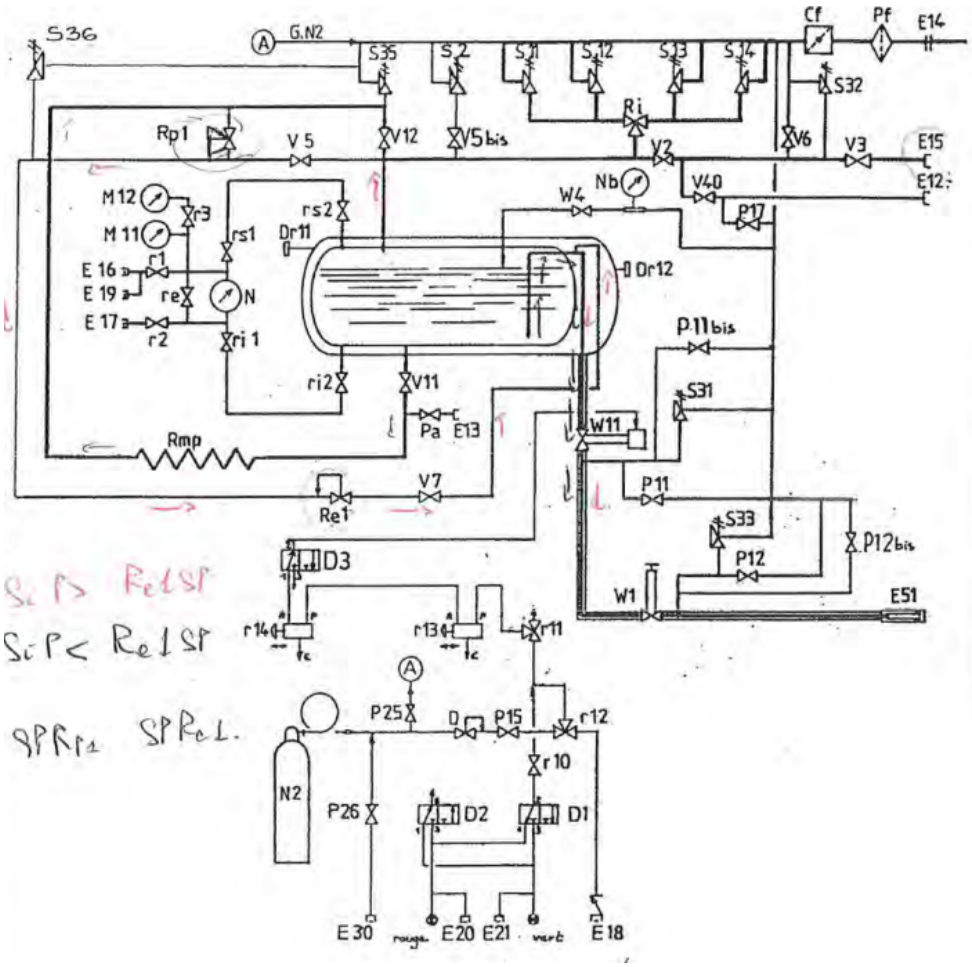

Figure 6.1: Tank flow diagram [38]

As Figure 6.1 shows, the flow will pass valves W11 and W1 before reaching E51, which is the connection to the hose. Here, in E51, the diameter changes from 40 to 50 mm. The increase in diameter will, conversely, increase the pressure by a small amount. There is no information about what kind of valves W11 and W1 are, but globe valves are currently the most used in applications using cryogenic fluids. These generally have a K-factor of 6 when fully open, which is quite low and can't explain the pressure loss on its own. All the other pipes and equipment around the main pipe are auxiliary systems, such as a nitrogen purging system and a pressure build-up system. These are not active while hydrogen is emptied from the tank so they will not influence the pressure. Potential pressure loss from the tank truck should be investigated further as it is the most common way of transporting cryogenic fuel for bunkering scenarios. The maintenance of pressure is a key parameter in the system to uphold the driving force between bunkering- and receiving vessel.

6.3.5 Pump vs pressure difference

Currently, it is most common to use a pressure difference to transfer fuel from bunkering vessels to receiving vessels in liquid hydrogen application. It is debated whether a pump is a better alternative, as it has its advantages such as removing the need to pressurize the tank truck. However, cavitation is a common problem in liquid hydrogen pumps. Cavitation happens when liquid going through the pump vaporizes and creates small bubbles. These bubbles implode as they pass the impeller creating vibrations and mechanical damage [39]. The combination of pressure and temperature where liquid hydrogen exists is quite small so a slight change in either can cause a phase transition. With today's technology, using a pressure difference as means of fuel transfer causes the least amount of problems.

6.4 Missing knowledge

This work has focused on theoretical analysis of experimental data using models. Much more research effort should be put into practical experimentation on the use of liquid hydrogen, and improvement of the knowledge and data available today. Below is a list of some of the knowledge holes that should be investigated:

1. The pressure loss in the beginning of the bunkering process from the truck.
2. The effect of phase transition on equipment and piping.
3. The assumption that liquid hydrogen is incompressible.

7 Conclusion

In this work, the ship bunkering process with liquid hydrogen has been investigated. The foundation of the work is based on experiments conducted by the Norwegian Defence Research Establishment (FFI) on liquid hydrogen release outside and inside a confined space. Calculations have been conducted using several models to compare with the experimental results.

Temperature readings from the experiments were compared to a Helmholtz free energy EOS solver that accurately calculates the thermodynamic state. The calculated values match the readings and the temperature development through the conducted tests. The authors of the FFI report state that the temperature sensors measured about 10°C higher than the actual temperature. This was not validated by the authors, but should be investigated further to accurately predict the hydrogen phase in the piping system.

An improved curve fitting using a second degree polynomial was used to increase the accuracy of the fitted pressure data from FFI. This gave a overall equal or better fit with slightly higher calculated mass flows.

When comparing the pipe pressure loss calculations to the pressure measured in the experiments, they are close to each other but varies in accuracy. This reinforces the assumption that liquid hydrogen can be considered incompressible in bunkering scenarios, but should be investigated further to check at what extent the assumption is valid. No clear results were shown for the origin of the large pressure drop at the start of the experiments, though this is believed to come from the tank truck.

An analysis of the hydrogen phase during a bunkering scenario has also been investigated. This analysis showed that liquid hydrogen will start to boil quickly after the bunkering begins due to the pressure loss.

Finally, the validity of the models used in this work is discussed followed by a brief overview of important aspects in liquid hydrogen bunkering. Hydrogen should be produced with a low carbon footprint to minimise the environmental impact. Furthermore, a fitting bunkering method should be chosen which depends on the location of the port, size of the port and available infrastructure. Lastly, the bunker system needs to have very low thermal conductivity throughout the system to ensure minimum boil-off.

References

[1] 'Primary energy: Statistical review of world energy (2021).' (2021), [Online]. Available: https://www.bp.com/en/global/corporate/energy-economics/statistical-review-of-world-energy/primary-energy.html.

[2] 'Burning of fossil fuels.' (), [Online]. Available: https://ugc.berkeley.edu/background-content/burning-of-fossil-fuels/.

[3] 'Iso 13600:(en) technical energy systems — basic concepts.' (1997), [Online]. Available: https://www.iso.org/obp/ui/#iso:std:iso:13600:ed-1:v1:en.

[4] 'European maritime transport environmental report,' European Maritime Safety Agency, European Environment Agency, 2021.

[5] 'Fourth greenhouse gas study 2020.' (), [Online]. Available: https://www.imo.org/en/OurWork/Environment/Pages/Fourth-IMO-Greenhouse-Gas-Study-2020.aspx.

[6] 'Hydrogen: A clean, flexible energy carrier.' (), [Online]. Available: https://www.energy.gov/eere/articles/hydrogen-clean-flexible-energy-carrier.

[7] 'Kawasaki hydrogen road: Hydrogen utilization.' (), [Online]. Available: https://global.kawasaki.com/en/hydrogen/.

[8] 'Fuel cells.' (), [Online]. Available: https://www.energy.gov/eere/fuelcells/fuel-cells.

[9] D. G. S. Research and Testing, 'Data report: Outdoor leakage studies,' Norwegian Defence Research Establishment, 2020.

[10] ——, 'Large scale leakage of liquid hydrogen (lh2)-tests related to bunkering and maritime use of liquid hydrogen,' Norwegian Defence Research Establishment, 2020.

[11] 'Hydrogen: Thermophysical properties.' (), [Online]. Available: https://www.engineeringtoolbox.com/hydrogen-d_1419.html.

[12] C. E. Brennen, *Fundamentals of Multiphase Flows*. Cambridge University Press, 2005.

[13] R. Agarwal and R. S. Dondapati, 'Numerical investigation on hydrodynamic characteristics of two-phase flow with liquid hydrogen through cryogenic feed lines at terrestrial and microgravity,' *Applied Thermal Engineering*, vol. 173, 2020.

[14] S. Mokhatab, W. Poe and J. Mak, *Handbook of Natural Gas Transmission and Processing*. Pearson, 2019.

[15] 'Slug flow.' (), [Online]. Available: https://en.wikipedia.org/wiki/Slug_flow.

[16] S. Mokhatab, J. V. Valappil, J. Y. Mak and D. A. Wood, *Handbook of Liquefied Natural Gas*. Elsevier, 2014.

[17] 'Explosive lessons in hydrogen safety.' (), [Online]. Available: https://www.nasa.gov/pdf/513855main_ASK_41s_explosive.pdf.

[18] 'First-aid procedures for cryogenic-induced injuries.' (), [Online]. Available: https://h2tools.org/bestpractices/first-aid-procedures-cryogenic-induced-injuries.

[19] D. A. Crowl and Y.-D. Jo, 'The hazards and risks of hydrogen,' *Journal of Loss Prevention in the Process Industries*, vol. 20, pp. 158–164, 2007.

[20] F. Wei and K. Tsuzaki, *Gaseous Hydrogen Embrittlement of Materials in Energy Technologies*. Woodhead Publishing, 2012.

[21] S. M. T. Forum, F. M. Design, L. C. AB, D. N. V. A. (DNV), L. GOT and W. S. AB, 'Lng ship to ship bunkering procedure,' Swedish Marine Technology Forum.

[22] 'Liquefied natural gas (lng) transfer and bunkering methods.' (), [Online]. Available: https://blog.dixonvalve.com/lng-transfer-and-bunkering-methods.

[23] 'Ship to ship bunkering.' (), [Online]. Available: https://www.gasum.com/en/sustainable-transport/maritime-transport/ship-to-ship-bunkering/.

[24] 'Number of ports with lng bunkering facilities worldwide in 2021, by region.' (), [Online]. Available: https://www.statista.com/statistics/1103931/lng-bunkering-availability-in-ports-by-region/.

[25] 'Lng bunker infrastructure.' (), [Online]. Available: https://sustainableworldports.org/clean-marine-fuels/lng-bunkering/ports/lng-bunker-infrastructure/#shore-to-ship.

[26] 'Small- and medium-scale lng terminals.' (), [Online]. Available: https://www.wartsila.com/docs/default-source/Power-Plants-documents/lng/small-and-medium-scale-lng-terminals_wartsila.pdf.

[27] M. Aziz, 'Liquid hydrogen: A review on liquefaction, storage, transportation, and safety,' *Energies*, vol. 14, no. 18, p. 5917, 2021.

[28] J. M. Smith, H. C. Van Ness, M. M. Abbott and M. T. Swihart, *Introduction to chemical engineering thermodynamics*. McGraw-Hill Education, 2018.

[29] M. Klell, 'Thermodynamics of gaseous and liquid hydrogen storage,' in *International Hydrogen Energy Congress and Exhibition*, ., 2007.

[30] J. Garche, C. K. Dyer, P. T. Moseley, Z. Ogumi, D. A. Rand and B. Scrosati, *Encyclopedia of electrochemical power sources*. Newnes, 2013.

[31] M. A. Shimko and P. M. Dunn, 'Combined reverse-brayton joule thompson hydrogen liquefaction cycle,' Gas Equipment Engineering Corporation, Milford, CT (United States), Tech. Rep., 2011.

[32] 'Vacuum jacketed insulation for lng pipe and hose.' (), [Online]. Available: http://hebb.org/lng-vacuum-insulation-small-pipe-LNGIndustry-reprint.pdf.

[33] T. Al-Shemmeri, *Engineering Fluid Mechanics*. bookboon, 2012.

[34] 'Thermodynamic models and tools for h2o, h2, co2 and air.' (2022), [Online]. Available: https://github.com/are-mj/thermodynamics/releases/tag/v2.1.

[35] 'Linest function.' (), [Online]. Available: https://support.microsoft.com/en-us/office/linest-function-84d7d0d9-6e50-4101-977a-fa7abf772b6d.

[36] D. A. Crowl and J. F. Louvar, *Chemical Process Safety: Fundamentals with Applications, 4th Edition*. Pearson, 2019.

[37] 'Thermophysical properties of fluid systems.' (), [Online]. Available: https://webbook.nist.gov/chemistry/fluid/.

[38] A. Liquid, *Container type cnt 45.000 litres lh2, 12bar, general data*, 1994.

[39] 'Pump cavitation and how to avoid it.' (), [Online]. Available: https://www.xylem.com/siteassets/support/case-studies/case-studies-pdf/cavitation-white-paper_final-2.pdf.

Appendix A

Models

A.1 Script with Helmholtz EOS

A.2 Phase analyser

A.3 Script for mass flow- and pressure calculation (Tests 1-4)

A.4 Excel documents read by Python (Test 1-4)

A.5 Nozzle calculator